E-Companion for "Production Management with General Demands and Lost Sales"

EC.1. Supplementary Materials for Section 4

EC.1.1. Proofs of Proposition 1 and Lemma 1

We prove that its Laplace transform solves the following equation for the conditional expected discounted cost until the first lost sales $c_{r,\rho}(u)$. For notational convenience, we omit the argument $r \geq 0$ in the related functions throughout this e-companion unless otherwise specified.

PROPOSITION EC.1. *The Laplace transform of $c_\rho(u)$, i.e., $\tilde{c}_\rho(u)$, satisfies the equation*

$$\psi(u) \cdot \tilde{c}_\rho(u) - \rho c_\rho(0) = -\tilde{g}(u), \quad u \geq 0, \tag{EC.1}$$

where $\psi(u)$ is the Lundberg equation defined by

$$\psi(u) := \rho u - r - \int_0^\infty (1 - e^{-ux})\nu(dx), \tag{EC.2}$$

and $\tilde{g}(\cdot)$ is the Laplace transform of $g(\cdot)$ with

$$g(u) := h(u) + \int_u^\infty w(x-u)\nu(dx). \tag{EC.3}$$

Proof of Proposition EC.1. By definition of $c_\rho(u)$ in (7), we know that it only accounts for the total cost incurred before the occurrence of the first lost sales. Therefore, in the analysis of $c_\rho(u)$, it is equivalent to assume that the inventory dynamics is

$$I(t) = I(0) + \rho t - D(t),$$

since we only focus on what happened before and exactly at the time of the first lost sales. We employ a family of processes $\{I_\epsilon(t), t \geq 0\}_{\epsilon>0}$ to approximate $\{I(t), t \geq 0\}$, which is defined as

$$I_\epsilon(t) := I(0) + \rho t - D_\epsilon(t), \tag{EC.4}$$

where $D_\epsilon(t)$ is a compound Poisson process with the jump intensity being

$$\lambda_\epsilon = \int_\epsilon^\infty \nu(dx) \tag{EC.5}$$

and the probability density function for each i.i.d. jump size being

$$f_\epsilon(x) = \frac{\pi(x)}{\int_\epsilon^\infty \nu(dx)} \mathbf{1}_{(\epsilon,\infty)}(x), \tag{EC.6}$$

where $\nu(dx) = \pi(x)dx$. Namely, if we only consider the jump whose size is larger than ϵ in the subordinator $D(t)$, we are dealing with a compound Poisson demand $D_\epsilon(t)$, where the corresponding Lévy measure is $\nu_\epsilon(dx) = \lambda_\epsilon f_\epsilon(x)dx = \nu(dx)\mathbf{1}_{(\epsilon,\infty)}(x)$. Lemma 2.1 in Morales (2007) states that $D_\epsilon(t)$ converges in distribution to $D(t)$, and therefore, I_ϵ converges weakly to I when ϵ goes to 0.

Denote the associated expected discounted cost until the first lost sales under inventory dynamics (EC.4) as $c_{\epsilon,\rho}(u)$. Using similar arguments as in the proof of Lemma 1 in Shi et al. (2014) or the proof of Theorem 3.1 in Cai et al. (2009), we can obtain the following expression for $c_{\epsilon,\rho}(u)$:

$$\begin{aligned} c_{\epsilon,\rho}(u) = &\int_0^\infty \lambda_\epsilon e^{-\lambda_\epsilon t} \int_0^t e^{-rs} h(u+\rho s) ds dt + \int_0^\infty \lambda_\epsilon e^{-(\lambda_\epsilon + r)t} \int_0^{u+\rho t} f_\epsilon(x) c_{\epsilon,\rho}(u+\rho t - x) dx dt \\ &+ \int_0^\infty \lambda_\epsilon e^{-(\lambda_\epsilon + r)r} \int_{u+\rho t}^\infty f_\epsilon(x) w(x-(u+\rho t)) dx dt. \end{aligned} \tag{EC.7}$$

The representation for $c_{\epsilon,\rho}(u)$ above implies that it is absolutely continuous. We can take a substitution of variables $y = u + \rho t$ and get

$$\begin{aligned} \rho c_{\epsilon,\rho}(u) = &\int_u^\infty e^{-\frac{\lambda_\epsilon + r}{\rho}(y-u)} h(y) dy + \int_u^\infty \lambda_\epsilon e^{-\frac{\lambda_\epsilon + r}{\rho}(y-u)} \int_0^y f_\epsilon(x) c_{\epsilon,\rho}(y-x) dx dy \\ &+ \int_u^\infty \lambda_\epsilon e^{-\frac{\lambda_\epsilon + r}{\rho}(y-u)} \int_y^\infty f_\epsilon(x) w(x-y) dx dy. \end{aligned} \tag{EC.8}$$

By taking the derivative with respect to u on both sides of (EC.8), we then obtain

$$\begin{aligned} \rho c'_{\epsilon,\rho}(u) = &-h(u) + \frac{\lambda_\epsilon + r}{\rho} \int_u^\infty e^{-\frac{\lambda_\epsilon + r}{\rho}(y-u)} h(y) dy \\ &- \int_0^u \lambda_\epsilon f_\epsilon(x) c_{\epsilon,\rho}(u-x) dx + \frac{\lambda_\epsilon + r}{\rho} \int_u^\infty e^{-\frac{\lambda_\epsilon + r}{\rho}(y-u)} \int_0^y \lambda_\epsilon f_\epsilon(x) c_{\epsilon,\rho}(y-x) dx dy \\ &- \int_u^\infty \lambda_\epsilon f_\epsilon(x) w(x-u) dx + \frac{\lambda_\epsilon + r}{\rho} \int_u^\infty e^{-\frac{\lambda_\epsilon + r}{\rho}(y-u)} \int_y^\infty \lambda_\epsilon f_\epsilon(x) w(x-y) dx dy \\ = &-h(u) - \int_0^u \lambda_\epsilon f_\epsilon(x) c_{\epsilon,\rho}(u-x) dx - \int_u^\infty \lambda_\epsilon f_\epsilon(x) w(x-u) dx + (\lambda_\epsilon + r) c_{\epsilon,\rho}(u). \end{aligned} \tag{EC.9}$$

We further take the Laplace transform with respect to u on both sides of (EC.9), which yields

$$\rho[u\tilde{c}_{\epsilon,\rho}(u) - c_{\epsilon,\rho}(0)] - (\lambda_\epsilon + r)\tilde{c}_{\epsilon,\rho}(u) + \lambda_\epsilon \tilde{f}_\epsilon(u)\tilde{c}_{\epsilon,\rho}(u) = -\tilde{g}_\epsilon(u), \quad u > 0,$$

where $g_\epsilon(u) := h(u) + \lambda_\epsilon \int_u^\infty f_\epsilon(x) w(x-u) dx$ for $u \geq 0$. After a simple rearrangement of terms, we have

$$\psi_\epsilon(u) \cdot \tilde{c}_{\epsilon,\rho}(u) - \rho c_{\epsilon,\rho}(0) = -\tilde{g}_\epsilon(u), \quad u > 0, \tag{EC.10}$$

where $\psi_\epsilon(\cdot)$ is the Lundberg equation associated with the process I_ϵ defined by

$$\psi_\epsilon(u) := \rho u - \lambda_\epsilon - r - \lambda_\epsilon \tilde{f}_\epsilon(u). \tag{EC.11}$$

The following lemma provides several important properties of the roots of the Lundberg equation $\psi_\epsilon(u) = 0$.

LEMMA EC.1. *For any $r > 0$, the Lundberg equation $\psi_\epsilon(u) = 0$ has a unique positive solution ξ_ϵ. Moreover, we have the following:*

(a) There is a bijection between ρ and ξ_ϵ, which is implicitly established by the equation

$$\rho = \frac{r}{\xi_\epsilon} + \lambda_\epsilon \tilde{F}_\epsilon(\xi_\epsilon), \tag{EC.12}$$

where $F(\cdot)$ is the complementary cumulative density function (CDF) of the distribution (EC.6)*.*

(b) The function $\xi_\epsilon(\rho)$ is strictly decreasing in ρ and satisfies

(i) $\lim_{\rho \to 0} \xi_\epsilon(\rho) = \infty$ *and* $\lim_{\rho \to 0} \rho \cdot \xi_\epsilon(\rho) = \lambda_\epsilon + r$*;*

(ii) $\lim_{\rho \to \infty} \xi_\epsilon(\rho) = 0$, *and* $\lim_{\rho \to \infty} \rho \cdot \xi_\epsilon(\rho) = r$*.*

Proof of Lemma EC.1. The existence of a unique positive solution to the Lundberg equation $\psi_\epsilon(u) = 0$ is a standard result following Gerber and Shiu (1997). The remaining claims come from Lemma 2 in Shi et al. (2014) and Kyprianou (2013). □

Based on the bijection between ρ and ξ_ϵ, we can derive the closed-form formulas for $c_{\epsilon,\rho}(0)$ and $\tilde{c}_{\epsilon,\rho}(u)$ in (EC.10).

LEMMA EC.2. *For $r > 0$ and $\rho > 0$, we have*

$$c_{\epsilon,\rho}(0) = \frac{1}{\rho} \tilde{g}_\epsilon(\xi_\epsilon) \text{ and } \tilde{c}_{\epsilon,\rho}(u) = \frac{\tilde{g}_\epsilon(\xi_\epsilon) - \tilde{g}_\epsilon(u)}{\psi_\epsilon(u)}, \text{ for } u \neq \xi_\epsilon. \tag{EC.13}$$

Proof of Lemma EC.2. Since ξ_ϵ is a solution to $\psi_\epsilon(u)=0$ and by letting $u=\xi$, we know from (EC.10) that $c_{\epsilon,\rho}(0)=\frac{1}{\rho}\tilde{g}_\epsilon(u)$. By plugging this back into (EC.10), we get the expression for $\tilde{c}_{\epsilon,\rho}(u)$ when $u\neq\xi_\epsilon$. $\square$

Meanwhile, since we already know that I_ϵ converges weakly to I, it is reasonable to expect that similar convergence results hold for the associated Lundberg equation, as shown in the following lemma.

LEMMA EC.3. *For any $r>0$, as ϵ goes to 0, the Lundberg equation $\psi_\epsilon(u)=0$ associated with I_ϵ converges to the Lundberg equation $\psi(u)=0$ of I, where $\psi(\cdot)$ is defined as*

$$\psi(u):=\rho u-r-\int_0^\infty(1-e^{-ux})\nu(dx).$$

Proof of Lemma EC.3. Using (EC.5) and (EC.6), we can rewrite (EC.11) as

$$\psi_\epsilon(u):=\rho u-r-\lambda_\epsilon\int_0^\infty(1-e^{-ux})f_\epsilon(x)dx=:\rho u-r-\Psi_{D_\epsilon}(u),$$

where $\Psi_{D_\epsilon}(\cdot)$ is the Laplace exponent of D_ϵ. Since $D_\epsilon\xrightarrow{d}D$, the corresponding Laplace exponent also converges. Therefore,

$$\psi_\epsilon(u)=\rho u-r-\Psi_{D_\epsilon}(u)\to\rho u-r-\Psi_D(u)=\rho u-r-\int_0^\infty(1-e^{-ux})\nu(dx)=\psi(u),$$

as $\epsilon\to0$, where $\Psi_D(u):=\int_0^\infty(1-e^{-ux})\nu(dx)$ is the Laplace exponent of D. $\square$

By Lemmas EC.1 and EC.3, the following lemma establishes the properties of the solutions to the Lundberg equation $\psi(u)=0$ for I as $\epsilon\to0$, proving Lemma 1.

LEMMA EC.4. *For any $r>0$, the Lundberg equation $\psi(u)=0$ has a unique positive solution ξ such that $\xi_\epsilon\to\xi$ as $\epsilon\to0$. Moreover, we have the following:*

(a) There is a bijection between ρ and ξ, which is implicitly established by the equation

$$\rho=\frac{r+\Psi_D(\xi)}{\xi}. \tag{EC.14}$$

(b) The function $\xi(\rho)$ is strictly decreasing in ρ and satisfies

(i) $\lim_{\rho\to 0}\xi(\rho)=\infty$ *and* $\lim_{\rho\to 0}\rho\cdot\xi(\rho)=\int_0^\infty \nu(dx)+r$*;*

(ii) $\lim_{\rho\to\infty}\xi(\rho)=0$, *and* $\lim_{\rho\to\infty}\rho\cdot\xi(\rho)=r$.

Proof of Lemma EC.4. The results are natural consequences of Lemma EC.1 and EC.3 by noting that $\lambda_\epsilon\to\int_0^\infty\nu(dx)$ when $\epsilon\to 0$. □

Consequently, combining the results of Proposition EC.2 and Lemma EC.4, we get

$$c_{\epsilon,\rho}(0)=\frac{1}{\rho}\tilde{g}_\epsilon(\xi_\epsilon)\to\frac{1}{\rho}\tilde{g}(\xi)=c_\rho(0) \tag{EC.15}$$

and

$$\tilde{c}_{\epsilon,\rho}(u)=\frac{\tilde{g}_\epsilon(\xi_\epsilon)-\tilde{g}_\epsilon(u)}{\psi_\epsilon(u)}\to\frac{\tilde{g}(\xi)-\tilde{g}(u)}{\psi(u)}=\tilde{c}_\rho(u), \tag{EC.16}$$

which implies (EC.1). We thus complete the proof of Proposition EC.1. □

Based on the equations (EC.15) and (EC.16), we have also proved Proposition 1.

EC.1.2. Proofs of Proposition 2 and Theorem 1

Throughout this section, we assume $r=0$ and omit the argument $r=0$ in related functions for the simplicity of arguments. We first state Lemmas EC.5-EC.9, which are used to prove Proposition 2 and Theorem 1.

LEMMA EC.5. *(a) The cycle times* $\{(\tau_{n+1}-\tau_n), n\geq 1\}$ *are independent identically distributed, and we have*

$$\mathbb{E}[\tau_1]=\varphi_u\geq\varphi_0=\mathbb{E}[\tau_{n+1}-\tau_n],\qquad n\geq 1.$$

(b) The costs over each cycle time $\{(C_\rho(\tau_{n+1})-C_\rho(\tau_n)), n\geq 1\}$ *are independent identically distributed, and we have*

$$\mathbb{E}[C_\rho(\tau_1)|I(0)=u]=c_\rho(u)\geq c_\rho(0)=\mathbb{E}[C_\rho(\tau_{n+1})-C_\rho(\tau_n)],\qquad n\geq 1.$$

Proof of Lemma EC.5. These results immediately follow from the strong Markov property and spatial homogeneity of the subordinator $D(t)$ as well as the inventory process $I(t)$ and the pathwise monotonicity of τ_1 as well as $I(t)$ in u. □

LEMMA EC.6. *Under the stability condition $\rho < \mu_\nu$, for any given large enough $T > 0$, with probability 1, we have*

$$\lim_{T\to\infty} m_T = \infty,$$

where $m_T := \sup\{m \in \mathbb{N}, \tau_m \le T\}$.

Proof of Lemma EC.6. By Lemmas EC.5 and EC.9, we know that for any $n \ge 1$, $\mathbb{E}[\tau_{n+1} - \tau_n] \le \mathbb{E}[\tau_1] < \infty$ under the stability condition. Let A_n be the event such that $\lim_{T\to\infty} m_T = n$. We then have

$$\mathbb{P}(A_n) = \mathbb{P}\{\tau_n - \tau_{n-1} = \infty\} = 0.$$

Therefore,

$$\mathbb{P}\left\{\lim_{T\to\infty} m_T = \infty\right\} = 1 - \mathbb{P}\left\{\bigcup_{n=1}^{\infty} A_n\right\} = 1 - \sum_{n=1}^{\infty} \mathbb{P}\{A_n\} = 1. \quad \square$$

LEMMA EC.7. *Under the stability condition $\rho < \mu_\nu$,*

$$\lim_{T\to\infty} \frac{m_T}{T} = \frac{1}{\varphi_0}, \quad a.s. \tag{EC.17}$$

and

$$\lim_{T\to\infty} \mathbb{E}\left[\frac{m_T}{T}\right] = \frac{1}{\varphi_0}. \tag{EC.18}$$

Proof of Lemma EC.7. We first show that

$$\lim_{T\to\infty} \frac{\tau_{m_T}}{T} = 1, \quad a.s. \tag{EC.19}$$

Based on our model formulation, $\tau_{i+1} - \tau_i$ are i.i.d. with bounded second moments. Therefore, for $1 < q \le 2$, an application of the Markov inequality gives

$$\sum_{i=1}^{\infty} \mathbb{P}\left(\left|\frac{\tau_{m_i+1} - \tau_{m_i}}{i} > \epsilon\right|\right) \le \sum_{i=1}^{\infty} \frac{1}{\epsilon^q} \mathbb{E}\left(\frac{\tau_{m_i+1} - \tau_{m_i}}{i}\right)^q = \sum_{i=1}^{\infty} \frac{\mathbb{E}(\tau_2 - \tau_1)^q}{(i\epsilon)^q} < \infty.$$

Therefore, by Borel-Cantelli lemma, $\lim_{T\in\mathbb{N}_+, T\to\infty} \frac{\tau_{m_T+1} - \tau_{m_T}}{T} = 0$ *a.s.*. Since $\lfloor T \rfloor \le T \le \lfloor T \rfloor + 1$, the same limiting result holds when T is a real sequence going to infinity. Then (EC.19) holds because

$$0 \le 1 - \lim_{T\to\infty} \frac{\tau_{m_T}}{T} \le \lim_{T\to\infty} \frac{\tau_{m_T+1} - \tau_{m_T}}{T} = 0.$$

Next, by Lemma EC.6, we know that $m_T \to \infty$ almost surely as $T \to \infty$, which implies, with probability 1,

$$\lim_{T\to\infty} \frac{\tau_{m_T}}{m_T} = \lim_{m\to\infty} \frac{\tau_m}{m} = \lim_{m\to\infty} \frac{\tau_1}{m} + \lim_{m\to\infty} \frac{1}{m} \sum_{i=1}^{m-1} (\tau_{i+1} - \tau_i) = \varphi_0, \tag{EC.20}$$

where the last equality follows from Proposition EC.5 and the law of large numbers. Therefore, combining (EC.19) and (EC.20) yields

$$\lim_{T\to\infty} \frac{m_T}{T} = \lim_{T\to\infty} \frac{m_T/\tau_{m_T}}{T/\tau_{m_T}} = \frac{1}{\varphi_0}, \quad a.s.$$

Moreover, to verify (EC.18), it suffices to show the uniform integrability of $\{m_T/T\}$. Let $\{\hat{\tau}_i\}$ be a i.i.d. sequence of indicator functions with $\hat{\tau}_i = \mathbf{1}_{\{\tau_{i+1}-\tau_i>1\}}$ for $i \in \mathbb{N}^+$. Clearly, we have $\sum_{i=1}^m \hat{\tau}_i \le \tau_m$. Define $\hat{m}_T = \sup\{m | \sum_{i=1}^m \hat{\tau}_i \le T\}$; it is then clear from the definition of $m_T := \sup\{m \in \mathbb{N} | \tau_m \le T\}$ that $m_T \le \hat{m}_T$. Let any m whenever $\tau_m \le T$, it implies that $\sum_{i=1}^m \hat{\tau}_i \le T$, so $\{m \in \mathbb{N} | \tau_m \le T\} \subseteq \{m | \sum_{i=1}^m \hat{\tau}_i \le T\}$, which further implies $m_T \le \hat{m}_T$. Denote $p = \mathbb{P}\{\tau_{i+1} - \tau_i > 1\}$, which is identical for all $i \in \mathbb{N}^+$, we know that $\hat{m}_T$ follows a negative binomial distribution with the respective parameters $\lfloor T \rfloor$ and $1-p$ based on the above discussion, which further gives

$$\mathbb{E}[m_T^2] \le \mathbb{E}[\hat{m}_T^2] = (\mathbb{E}[\hat{m}_T])^2 + Var(m_T) = \frac{\lfloor T \rfloor (\lfloor T \rfloor + 1) - \lfloor T \rfloor (1-p)}{(1-p)^2} \le C_1 T + C_2 T^2,$$

where C_1 and C_2 are both constants, clearly independent of T. Therefore, by Markov's inequality, we have

$$\mathbb{P}\left(\frac{m_T}{T} \ge x\right) \le \frac{\mathbb{E}[m_T^2]}{T^2 x^2} \le \frac{C}{x^2},$$

which completes the proof. □

Lemma EC.8. *Under the stability condition $\rho < \mu_\nu$, we have*

$$\lim_{T\to\infty} \frac{1}{T} \mathbb{E}\left[C_\rho(\tau_1)\right] = 0.$$

Proof of Lemma EC.8. It suffices to show that $\mathbb{E}\left[C_\rho(\tau_1)\right]$ is finite. Since $w(x)$ is an increasing concave function, there exist some constants $b_1, b_2 \ge 0$ such that $w(x) \le b_1 x + b_2$, we have

$$\int_0^t w(dL(z)) \le w\left(\int_0^t dL(z)\right) = w(L_t) \le b_1 L_t + b_2 \le b_1 D(t) + b_2.$$

Notice that for any $t \geq 0$, $I(t) \leq u + \rho t$, and h is an increasing concave function, which means that

$$\begin{aligned} C_\rho(t) &= \int_0^t h(I(z))dz + \int_0^t w(dL(z)) \\ &\leq \int_0^t h(u+\rho z)dz + w(L_t) \\ &\leq h(u)t + \frac{1}{2}h'(u)\rho t^2 + b_1 D(t) + b_2. \end{aligned}$$

Therefore, we obtain

$$\begin{aligned} \mathbb{E}\left[C_\rho(\tau_1)\right] &= \mathbb{E}\{\mathbb{E}\left[C_\rho(\tau_1)|\tau_1\right]\} \\ &\leq \mathbb{E}[h(u)\tau_1 + \frac{1}{2}h'(u)\rho\tau_1^2 + b_1 D(\tau_1) + b_2] \\ &= h(u)\mathbb{E}[\tau_1] + \frac{1}{2}h'(u)\rho\mathbb{E}[\tau_1^2] + b_1\mathbb{E}[D(\tau_1)] + b_2 \\ &< \infty, \end{aligned}$$

where $D(\tau_1)$ is bounded by $u + \rho\tau_1$ plus the amount of the first lost sales, and hence it has a finite expectation. □

LEMMA EC.9. *Under the stability condition $\rho < \mu_\nu$, τ_1 has finite j-th moments for any $j > 0$.*

Proof of Lemma EC.9. The result follows simply from showing that the j-th order derivative of the Laplace transform of τ_1 at 0 is finite; see Theorem 8.1 in Kyprianou (2014). □

Proof of Proposition 2. Let m_T be a random integer such that $\tau_{m_T} \leq T \leq \tau_{m_T+1}$ for a large enough T. We then have

$$\begin{aligned} F_\rho &= \lim_{T\to\infty} \frac{1}{T}\mathbb{E}[C_\rho(T)] \\ &= \lim_{T\to\infty} \frac{1}{T}\mathbb{E}\left[C_\rho(\tau_1) + \sum_{i=2}^{m_T}(C_\rho(\tau_i) - C_\rho(\tau_{i-1})) + (C_\rho(T) - C_\rho(\tau_{m_T}))\right] \end{aligned} \tag{EC.21}$$

For the first term in (EC.21), by Lemma EC.8, we have

$$\lim_{T\to\infty} \frac{1}{T}\mathbb{E}[C_\rho(\tau_1)] = 0. \tag{EC.22}$$

For the second term, by Lemmas EC.5 and EC.7, we know from the strong Markov property,

$$\begin{aligned}
&\lim_{T\to\infty}\frac{1}{T}\mathbb{E}\left[\sum_{i=2}^{m_T}(C_\rho(\tau_i)-C_\rho(\tau_{i-1}))\right]\\
&=\lim_{T\to\infty}\frac{1}{T}\mathbb{E}\left[(m_T-1)(C_\rho(\tau_2)-C_\rho(\tau_1))\right]\\
&=\lim_{T\to\infty}\frac{(m_T-1)}{T}\cdot\mathbb{E}\left[(C_\rho(\tau_2)-C_\rho(\tau_1))\right]=\frac{c_\rho(0)}{\varphi_0},
\end{aligned}\tag{EC.23}$$

where the second equality follows from the dominated convergence theorem together with the uniform integrability of $\{m_T/T\}$ as shown in Lemma EC.7. Lastly, for the third term in (EC.21), we obtain from Lemma EC.5 that

$$\begin{aligned}
0&\le\lim_{T\to\infty}\frac{1}{T}\mathbb{E}[C_\rho(T)-C_\rho(\tau_{m_T})]\\
&\le\lim_{T\to\infty}\frac{1}{T}\mathbb{E}[C_\rho(\tau_{m_T+1})-C_\rho(\tau_{m_T})]\\
&\le\lim_{T\to\infty}\frac{1}{T}\mathbb{E}[C_\rho(\tau_1)]=0,
\end{aligned}\tag{EC.24}$$

since $\tau_{n+1}-\tau_n\overset{d}{\le}\tau_1$ for every n. From (EC.22), (EC.23), and (EC.24), we conclude that

$$F_\rho=\lim_{T\to\infty}\frac{1}{T}\mathbb{E}[C_\rho(T)]=\frac{c_\rho(0)}{\varphi_0}=a_0.\quad\square\tag{EC.25}$$

Proof of Theorem 1. Using a standard martingale approach, one can follow Kella and Whitt (1992) to derive the formula for the expected cycle time φ_0 under the stability condition $\rho<\mu_\nu$ as

$$\varphi_0=\frac{1}{\rho\xi_0},$$

where $\xi_0>0$ is the unique positive solution of the Lundberg equation $\rho u-\int_0^\infty(1-e^{-ux})\nu(dx)=0$. Therefore, from (8) and (EC.25), we know

$$F_\rho=a_0=\xi_0\tilde{g}(\xi_0).$$

The optimal rate ρ_0^* can be derived by first minimizing F_ρ as a function in ξ_0 and then transforming back to ρ via the bijection established in Lemma 1. $\square$

EC.1.3. Proof of Theorem 2

As the first step, we notice that by the strong Markov property of the inventory process (2), we can link the total conditional discounted cost $\Phi_\rho(u)$ in (6) with the discounted cost until the first lost-sales $c_\rho(u)$ in (7) via the following proposition.

PROPOSITION EC.2. *For any initial inventory $u \geq 0$, we have*

$$\Phi_\rho(u) = c_\rho(u) + d_\rho(u)\Phi_\rho(0), \tag{EC.26}$$

where $d_\rho(u)$ is the discount factor of the first occurrence of lost sales defined by

$$d_\rho(u) := \mathbb{E}\left[e^{-r\tau_1}\middle| I(0) = u\right]. \tag{EC.27}$$

Proof of Proposition EC.2. This directly follows from the strong Markov property of the inventory process $I(t)$ in (2) and some standard arguments. □

In other words, Proposition EC.2 states that the total cost can be separated into two parts under the strong Markov property: the first part is the cost incurred from the initial inventory level to the occurrence of the first lost sales, and the remaining part is simply the cost incurred when starting from the zero initial inventory. To this end, to investigate the target cost objective function $\Phi_\rho(u)$, it suffices to analyze the other two terms $c_\rho(u)$ and $d_\rho(u)$, since $\Phi_\rho(0)$ can be solved endogenously in (EC.26) by setting $u = 0$ on its both sides.

Notably, according to the definition in (EC.27), $d_\rho(u)$ can be regarded as a particular case of $c_\rho(u)$ by letting $h(\cdot) \equiv 0$ and $w(\cdot) \equiv 1$ in (4) and (7). To this end, we are able to derive the explicit expressions for $\tilde{d}_\rho(u)$ and $\tilde{\Phi}_\rho(u)$ based on the results of Proposition 1, which also completes the proof of Theorem 2.

PROPOSITION EC.3. *For any $r > 0$ and $\rho > 0$,*

(a) the Laplace transform of the discount factor of the first occurrence of lost sales is

$$\tilde{d}_\rho(u) = \frac{r}{\psi(u)}\left[\frac{1}{u} - \frac{1}{\xi}\right] + \frac{1}{u}, \text{ for } u \neq \xi, \quad \text{and} \quad d_\rho(0) = 1 - \frac{r}{\rho\xi};$$

(b) the Laplace transform of the total conditional expected discounted cost is

$$\tilde{\Phi}_\rho(u) = \xi\tilde{g}(u)\frac{r + \psi(u)}{ru\psi(u)} - \frac{\tilde{g}(u)}{\psi(u)}, \text{ for } u \neq \xi, \quad \text{and} \quad \Phi_\rho(0) = \frac{\xi}{r}\tilde{g}(\xi).$$

Proof of Proposition EC.3. (a) We know that $d_\rho(u)$ is a special case of $c_\rho(u)$ if we set $h(\cdot)\equiv 0$ and $w(\cdot)\equiv 1$ in (4) and (7). Therefore, in this setting,

$$\begin{aligned}\tilde{g}(x) &= \int_0^\infty e^{-xu} g(u)du = \int_0^\infty e^{-xu}\int_u^\infty \nu(dy)du \\ &= \int_0^\infty \int_0^y e^{-xu}du\nu(dy) = \int_0^\infty \frac{1}{x}(1-e^{-xy})\nu(dy) \\ &= \frac{\Psi_D(x)}{x}.\end{aligned}$$

By Proposition 1 and the LPR ξ such that $\psi(\xi)=0$, we have

$$d_\rho(0) = \frac{1}{\rho}\frac{\Psi_D(\xi)}{\xi} = \frac{\rho\xi - r}{\rho\xi} = 1 - \frac{r}{\rho\xi},$$

and

$$\begin{aligned}\tilde{d}_\rho(u) &= \frac{\frac{\Psi_D(\xi)}{\xi} - \frac{\Psi_D(u)}{u}}{\psi(u)} = \frac{\rho - \frac{r}{\xi} - \frac{\rho u - r - \psi(u)}{u}}{\psi(u)} \\ &= \frac{r}{\psi(u)}\left[\frac{1}{u} - \frac{1}{\xi}\right] + \frac{1}{u}.\end{aligned}$$

(b) In (EC.26), letting $u=0$ on both sides yields

$$\Phi_\rho(0) = c_\rho(0) + d_\rho(0)\Phi_\rho(0),$$

which implies that

$$\Phi_\rho(0) = \frac{c_\rho(0)}{1-d_\rho(0)} = \frac{\frac{1}{\rho}\tilde{g}(\xi)}{1-(1-\frac{r}{\rho\xi})} = \frac{\xi}{r}\tilde{g}(\xi).$$

Furthermore, taking the Laplace transform with respect to u on both sides of (EC.26), we have

$$\begin{aligned}\tilde{\Phi}_\rho(u) &= \tilde{c}_\rho(u) + \tilde{d}_\rho(u)\Phi_\rho(0) = \frac{\tilde{g}(\xi)-\tilde{g}(u)}{\psi(u)} + \left[\frac{r}{\psi(u)}\left(\frac{1}{u}-\frac{1}{\xi}\right)+\frac{1}{u}\right]\cdot\frac{\xi}{r}\tilde{g}(\xi) \\ &= -\frac{\tilde{g}(u)}{\psi(u)} + \frac{\xi\tilde{g}(\xi)(r+\psi(u))}{ru\psi(u)}, \text{ for } u\neq\xi. \quad \square\end{aligned}$$

EC.1.4. Proof of Proposition 3

We first rewrite $\tilde{\Phi}_\rho(u)$ in Theorem 2 as,

$$\tilde{\Phi}_\rho(z) = \frac{\xi\tilde{g}(\xi)}{r}\frac{1}{z} + \left[\frac{\xi\tilde{g}(\xi)}{z} - \tilde{g}(z)\right]\cdot\frac{1}{\psi(z)}. \tag{EC.28}$$

Let $\eta_\xi(u)$ be the inverse Laplace transform of $\frac{1}{\psi(z)}$ at u. After taking the inverse Laplace transforms on both sides of (EC.28), we obtain the renewal-type representation for $\Phi_\xi(u)$:

$$\Phi_\xi(u) = \frac{\xi\tilde{g}(\xi)}{r} + [G_\xi * \eta_\xi](u) = \Phi_\xi(0) + [G_\xi * \eta_\xi](u), \tag{EC.29}$$

where $*$ denotes the convolution operator so that $[G_\xi * \eta_\xi](u) := \int_0^t G_\xi(w)\eta_\xi(t-w)dw$ and $G_\xi(u)$ is defined by

$$G_\xi(x) := \xi\tilde{g}(\xi) - g(x). \tag{EC.30}$$

It then suffices to solve for $\eta_\xi(u)$. By definition, the inverse Laplace transform of $\frac{1}{\psi(z)}$ is

$$\eta_\xi(u) = \mathcal{L}^{-1}\left[\frac{1}{\psi(z)}\right](u) = \lim_{R\to\infty}\frac{1}{2\pi i}\int_{\gamma-iR}^{\gamma+iR} e^{zu}\frac{1}{\psi(z)}dz,$$

where $\gamma > \xi$. Define S_R as the left semicircle with radius $R > \gamma - \theta$ centered at $(\gamma, 0)$, L_R as the straight line connecting $(\gamma, \gamma - iR)$ and $(\gamma, \gamma + iR)$, and C_R as the counterclockwise closed curve $S_R \cup L_R$; see plot of the left semicircle.

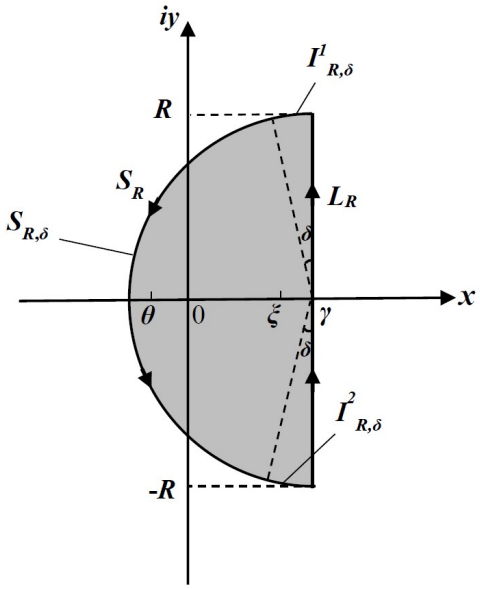

Then we have

$$\begin{aligned}\eta_\xi(u) &= \lim_{R\to\infty}\frac{1}{2\pi i}\int_{\gamma-iR}^{\gamma+iR} e^{zu}\frac{1}{\psi(z)}dz \\ &= \lim_{R\to\infty}\frac{1}{2\pi i}\left[\int_{C_R} e^{zu}\frac{1}{\psi(z)}dz - \int_{S_R} e^{zu}\frac{1}{\psi(z)}dz\right].\end{aligned} \tag{EC.31}$$

By the classical residue theorem, we have

$$\int_{C_R} e^{zu}\frac{1}{\psi(z)}dz = 2\pi i\left[\frac{e^{\xi u}}{\psi'(\xi)} + \frac{e^{\theta u}}{\psi'(\theta)}\right],$$

while the second term in (EC.31), $\int_{S_R} e^{zu}\frac{1}{\psi(z)}dz$, vanishes as $R\to\infty$ for any $u > 0$, and we prove this in what follows. Denote $z = \gamma + Re^{i\theta}$, $\frac{\pi}{2} \le \theta \le \frac{3\pi}{2}$, and let us separate the semicircle into different

portions. Define $\delta > 0$, and $S_{R,\delta}$ to be the arc where $\theta \in (\frac{\pi}{2}+\delta, \frac{3\pi}{2}-\delta)$. Correspondingly, define $I_{R,\delta}$ to be the remaining part of the semicircle, which includes both the upper and lower sections, and we respectively denote them by $I^1_{R,\delta}$ which refers to the area where $\theta \in [\frac{\pi}{2}, \frac{\pi}{2}+\delta]$, and $I^2_{R,\delta}$ which refers to the area where $\theta \in [\frac{3\pi}{2}-\delta, \frac{3\pi}{2}]$.

Given an arbitrarily small $\delta > 0$, we first consider the following integral:

$$\left| \int_{I^1_{R,\delta}} e^{zu} \frac{1}{\psi(z)} dz \right| \leq \delta R \left| \sup_{\theta \in [\frac{\pi}{2}, \frac{\pi}{2}+\delta]} e^{(\gamma + Ru\cos\theta)} \frac{1}{\psi(z)} \right|.$$

For $\theta \in [\frac{\pi}{2}, \frac{\pi}{2}+\delta]$, $\cos\theta \leq 0$, hence the term $e^{R\cos\theta u}$ is bounded by 1 even as $R \to \infty$. Next, we study the behavior of $\psi(z)$ near the point $\theta = \frac{\pi}{2}+\delta$, particularly at that point, such that for $z = \gamma + Re^{i(\frac{\pi}{2}+\delta)}$,

$$\begin{aligned}
\psi(z) &= \rho z - r - \int_0^\infty \left(1 - e^{-zx}\right) \nu(dx) \\
&= \rho(\gamma + Re^{\frac{i\pi}{2}+i\delta}) - r - \int_0^\infty \left(1 - e^{-x(\gamma + Re^{\frac{i\pi}{2}+i\delta})}\right) \nu(dx) \\
&= \rho(\gamma + iR(\cos\delta + i\sin\delta)) - r - \int_0^\infty \left(1 - e^{-x(\gamma + iR(\cos\delta + i\sin\delta))}\right) \nu(dx).
\end{aligned}$$

As δ gets closer to 0, the term $iR(\cos\delta + i\sin\delta)$ is dominated by $iR\cos\delta$, and hence is of the order $O(R)\cdot i$. As for the integrand in the last term, namely $1 - e^{-x\gamma}e^{-xiR\cos\delta}e^{xR\sin\delta}$, we have $e^{-x\gamma} < 1$ and $|e^{-xiR\cos\delta}| = 1$, while $e^{xR\sin\delta}$ increases with R. To this end, we have $\psi(\gamma + Re^{i(\frac{\pi}{2}+\delta)}) = O(R)\cdot i + O(g(R))$, where $g(R)$ is some positive increasing function of quadratic growth in R, and hence $|\psi(\gamma + Re^{i(\frac{\pi}{2}+\delta)})| \geq O(R)$. By uniform continuity, we have the same conclusion for all $\theta \in [\frac{\pi}{2}, \frac{\pi}{2}+\delta]$ uniformly, and hence $\left|\int_{I^1_{R,\delta}} e^{zu}\frac{1}{\psi(z)}dz\right|$ is bounded by $\delta O(1)$, as

$$\left| \int_{I^1_{R,\delta}} e^{zu} \frac{1}{\psi(z)} dz \right| \leq \delta R \left| \sup_{\theta \in [\frac{\pi}{2}, \frac{\pi}{2}+\delta]} e^{(\gamma + R\cos\theta u)} \frac{1}{\psi(z)} \right| \leq \frac{\delta R}{O(R)} = \delta O(1).$$

Similarly, $\left|\int_{I^2_{R,\delta}} e^{zu}\frac{1}{\psi(z)}dz\right|$ is also bounded by $\delta O(1)$.

Finally, for the integral over $S_{R,\delta}$, we have

$$\begin{aligned}
\left| \int_{S_{R,\delta}} e^{zu} \frac{1}{\psi(z)} dz \right| &= \left| \int_{S_{R,\delta}} e^{(\gamma u + R(e^{i\theta})u)} \frac{1}{\psi(z)} iRe^{i\theta} d\theta \right| \\
&= \left| \int_{S_{R,\delta}} e^{\gamma u + Ru\cos\theta + iRu\sin\theta + i\theta} \frac{1}{\psi(z)} R d\theta \right| \\
&= \left| \int_{S_{R,\delta}} e^{\gamma u} e^{Ru\cos\theta} e^{i\theta} e^{iRu\sin\theta} \frac{1}{\psi(z)} R d\theta \right|.
\end{aligned}$$

We then investigate these factors one by one. Recall that $\cos\theta<0$ for $\theta\in(\frac{\pi}{2}+\delta,\frac{3\pi}{2}-\delta)$. Particularly, $-\cos\theta\geq-\cos\left(\frac{\pi}{2}+\delta\right)=\sin\delta$, and we have $e^{Ru\cos\theta}\to 0$ uniformly as $R\to\infty$; furthermore, $\left|e^{i\theta}\right|=\left|e^{iRu\sin\theta}\right|=1$. As for $\frac{1}{\psi(z)}$, for any small enough $\delta>0$,

$$\left|\sup_{\theta\in\left[\frac{\pi}{2},\frac{3\pi}{2}\right]}\frac{1}{\psi(z)}-\sup_{\theta\in\left(\frac{\pi}{2}+\delta,\frac{3\pi}{2}-\delta\right)}\frac{1}{\psi(z)}\right|\leq\frac{1}{O(R)}.$$

As a result, we can fix a δ_0, and by uniform continuity of $\frac{1}{\psi(z)}$,

$$\left|\sup_{\theta\in\left(\frac{\pi}{2}+\delta_0,\frac{3\pi}{2}-\delta_0\right)}\frac{1}{\psi(z)}\right|\leq C.$$

Therefore, for any δ, we have

$$\left|\sup_{\theta\in\left(\frac{\pi}{2}+\delta,\frac{3\pi}{2}-\delta\right)}\frac{1}{\psi(z)}\right|\leq\left|\sup_{\theta\in\left[\frac{\pi}{2},\frac{3\pi}{2}\right]}\frac{1}{\psi(z)}\right|\leq\frac{1}{O(R)}+C.$$

All these facts lead to

$$\left|\int_{S_R,\delta}e^{zu}\frac{1}{\psi(z)}dz\right|\leq R\pi e^{-Ru\sin\delta}\left(\frac{1}{O(R)}+C\right)\to 0\quad\text{ as }\quad R\to\infty.$$

Consequently,

$$\begin{aligned}&\limsup_{R\to\infty}\left|\int_{S_R}e^{zu}\frac{1}{\psi(z)}dz\right|\\&\leq\lim_{R\to\infty}\left|\int_{S_{R,\delta}}e^{zu}\frac{1}{\psi(z)}dz\right|+\limsup_{R\to\infty}\left|\int_{I^1_{R,\delta}}e^{zu}\frac{1}{\psi(z)}dz\right|+\limsup_{R\to\infty}\left|\int_{\substack{1\\R,\delta}}e^{zu}\frac{1}{\psi(z)}dz\right|\\&=2\delta O(1).\end{aligned}$$

Hence, $\lim_{R\to\infty}\left|\int_{S_R}e^{zu}\frac{1}{\psi(z)}dz\right|=0$ given any arbitrarily small $\delta>0$.

Consequently, we know

$$\eta_\xi(u)=\frac{e^{\xi u}}{\psi'(\xi)}+\frac{e^{\theta u}}{\psi'(\theta)}.\tag{EC.32}$$

Finally, substituting (EC.30) and (EC.32) into (EC.29) implies (11).

EC.1.5. Proof of Proposition 4

Note that the following identity holds

$$c_\rho(u)=e^{ku}\bar{c}_\rho(u).\tag{EC.33}$$

We follow the procedure of Theorem EC.1 in Section EC.1.1 to derive the explicit expressions in Proposition 4. Specifically, Substituting $c_{\epsilon,\rho}(u) = e^{ku}\bar{c}_{\epsilon,\rho}(u)$ into (EC.9), we have the integro-differential equation for $\bar{c}_{\epsilon,\rho}(u) := e^{-ku}c_{\epsilon,\rho}(u)$,

$$\rho e^{ku}\bar{c}'_{\epsilon,\rho}(u)+\rho k e^{ku}\bar{c}_{\epsilon,\rho}(u) = -h(u)-\int_0^u \lambda_\epsilon f_\epsilon(x)e^{k(u-x)}\bar{c}_{\epsilon,\rho}(u-x)dx-\int_u^\infty \lambda_\epsilon f_\epsilon w(x-u)dx+(\lambda_\epsilon+r)e^{ku}\bar{c}_{\epsilon,\rho}(u).$$

Dividing both sides by e^{ku}, we have

$$\rho\bar{c}'_{\epsilon,\rho}(u)+\rho k\bar{c}_{\epsilon,\rho}(u) = -\int_0^u \lambda_\epsilon f_\epsilon(x)e^{-kx}\bar{c}_{\epsilon,\rho}(u-x)dx-\bar{g}_\epsilon(u)+(\lambda_\epsilon+r)\bar{c}_{\epsilon,\rho}(u), \tag{EC.34}$$

where we set $\bar{g}_\epsilon(u) := e^{-ku}g_\epsilon(u)$. We further take the Laplace transform of both sides in (EC.34), and after a simple rearrangement of terms, we obtain

$$\psi_\epsilon(u+k)\cdot\tilde{\bar{c}}_{\epsilon,\rho}(u)-\rho c_{\epsilon,\rho}(0) = -\tilde{\bar{g}}_\epsilon(u), \quad u>0.$$

The remaining approximation procedures are the same as those in the proof of Proposition EC.1, and one can finally derive that the Laplace transform of $\bar{c}_\rho(u)$ is given by $c_\rho(0) = \frac{1}{\rho}\cdot\tilde{\bar{g}}(\zeta)$ and

$$\tilde{\bar{c}}_\rho(u) = \frac{\tilde{\bar{g}}(u)-\tilde{\bar{g}}(\zeta)}{\psi(u+k)}, \text{ for } u\in\{a+bi : a\geq 0, b\in\mathbb{R}\}\backslash\{0,\zeta\}, \tag{EC.35}$$

where $\tilde{\bar{g}}(\cdot)$ is the Fourier transform of $\bar{g}(u) := e^{-ku}g(u)$. Furthermore, a similar argument as in the proof of Proposition EC.3 can lead to the claim in Proposition 4. We finally remark that since $\zeta := \xi - k$ with k being a fixed positive constant, there is a bijection between ζ and ρ by Lemma EC.4(a).

EC.1.6. Expressions for $\tilde{\bar{g}}(u)$ with special penalty functions $w(\cdot)$

Recall the definition of $g(\cdot)$ in (10). Set $\bar{h}(u) := e^{-ku}h(u)$ and

$$\begin{aligned}\tilde{\bar{g}}(u) &= \int_0^\infty e^{-(u+k)z}\left(h(z)+\int_z^\infty w(x-z)\nu(dx)\right)dz = \tilde{\bar{h}}(u)+\int_0^\infty\int_0^x e^{-(u+k)z}w(x-z)dz\nu(dx)\\ &= \tilde{\bar{h}}(u)+\int_0^\infty e^{-(u+k)x}\int_0^x e^{(u+k)z}w(z)dz\nu(dx).\end{aligned}$$

(a) If the penalty cost function $w(\cdot)$ is a fixed constant, i.e., $w(x)=K_0\geq 0$, meaning that whenever a sale is lost regardless of its size, we always impose a constant penalty in the objective function. Then,

$$\tilde{\bar{g}}(u)=\tilde{\bar{h}}(u)+K_0\int_0^\infty e^{-(u+k)x}\int_0^x e^{(u+k)z}dz\nu(dx)=\tilde{\bar{h}}(u)+\frac{K_0}{u+k}\Psi_D(u+k). \tag{EC.36}$$

(b) If the penalty $w(\cdot)$ is linear, i.e., $w(x)=K_1x$, where the penalty cost incurred by lost sales is proportional to its size, then

$$\begin{aligned}\tilde{\bar{g}}(u)&=\tilde{\bar{h}}(u)+K_1\int_0^\infty e^{-(u+k)x}\int_0^x ze^{(u+k)z}dz\nu(dx)=\tilde{\bar{h}}(u)+\frac{K_1}{(u+k)^2}\int_0^\infty e^{-(u+k)x}-1+(u+k)x\nu(dx)\\&=\tilde{\bar{h}}(u)+\frac{K_1\mu_\nu}{u+k}-\frac{K_1}{(u+k)^2}\Psi_D(u+k).\end{aligned} \tag{EC.37}$$

(c) For some other nonlinear forms of the penalty cost function $w(\cdot)$, sometimes it is still possible to derive the explicit expression for $\tilde{\bar{g}}(u)$; for instance, $w(x)=K_2(1-e^{-\delta x})$. It implies that the penalty increases with the lost-sales size with a diminishing marginal cost, and it is uniformly bounded by $K_2\geq 0$. Then we have

$$\begin{aligned}\tilde{\bar{g}}(u)&=\tilde{\bar{h}}(u)+K_2\int_0^\infty e^{-(u+k)x}\int_0^x e^{(u+k)x}(1-e^{-\delta x})dz\nu(dx)\\&=\tilde{\bar{h}}(u)+\frac{K_2\Psi_D(u+k)}{u+k}+K_2\int_0^\infty e^{-\xi x}\int_0^x e^{u+k-\delta}dz\nu(dx)\\&=\tilde{\bar{h}}(u)+\frac{K_2\Psi_D(u+k)}{u+k}+K_2\frac{\Psi_D(u+k)-\Psi_D(\delta)}{u+k-\delta},\quad \text{for } u\neq\delta-k.\end{aligned} \tag{EC.38}$$

In particular,

$$\begin{aligned}\tilde{\bar{g}}(\delta-k)&=\tilde{\bar{h}}(\delta-k)+K_2\int_0^\infty e^{-\delta x}\int_0^x e^{\delta x}(1-e^{-\delta x})dz\nu(dx)\\&=\tilde{\bar{h}}(\delta-k)+\frac{K_2\Psi_D(\delta)}{\delta}+K_2\int_0^\infty xe^{-\delta x}\nu(dx)\\&=\tilde{\bar{h}}(\delta-k)+\frac{K_2\Psi_D(\delta)}{\delta}+K_2\Psi'_D(\delta),\end{aligned} \tag{EC.39}$$

where the last equation follows from an interchange in the order of differentiation and integration.

EC.1.7. Error Analysis in Computing $\Phi_\rho(u)$ Using Fourier-cosine Method

We know from (17) that two different errors - *replacement error* η_1 and *truncation error* η_2 - are incurred in our Fourier-cosine method. We aim to give explicit bounds on these two errors in terms of the approximation parameters and study the corresponding convergence rates. To begin with, we have the following expression for the *replacement error* η_1.

PROPOSITION EC.4. *The replacement error* η_1 *can be expressed as*

$$\eta_1 = -\sum_{n=1}^{\infty} e^{-2akn} \left[\Phi_\rho(2na+u) + e^{2ku}\Phi_\rho(2na-u)\right].$$

Proof of Proposition EC.4. When $m=2n-1$, $n\geq 1$, we have

$$\begin{aligned}\sum_{j=0}^{\infty}{}' \frac{2}{a}\Re\left\{\int_{ma}^{(m+1)a} \bar{\Phi}_\rho(z)e^{i\frac{j\pi}{a}z}dz\right\}\cos\left(\frac{j\pi}{a}u\right) &= \sum_{j=0}^{\infty}{}' \frac{2}{a}\int_{-a}^{0} \bar{\Phi}_\rho(2na+z)\cos\left(\frac{j\pi}{a}z\right)dz\cos\left(\frac{j\pi}{a}u\right)\\ &= \sum_{j=0}^{\infty}{}' \frac{2}{a}\int_{0}^{a} \bar{\Phi}_\rho(2na-z)\cos\left(\frac{j\pi}{a}z\right)dz\cos\left(\frac{j\pi}{a}u\right)\\ &= \bar{\Phi}_\rho(2na-u),\end{aligned}$$

where the last equation follows from the cosine series expansion formula. Similarly, when $m=2n$, $n\geq 1$, we have

$$\begin{aligned}\sum_{j=0}^{\infty}{}' \frac{2}{a}\Re\left\{\int_{ma}^{(m+1)a} \bar{\Phi}_\rho(z)e^{i\frac{j\pi}{a}z}dz\right\}\cos\left(\frac{j\pi}{a}u\right) &= \sum_{j=0}^{\infty}{}' \frac{2}{a}\int_{0}^{a} \bar{\Phi}_\rho(2na+z)\cos\left(\frac{j\pi}{a}z\right)dz\cos\left(\frac{j\pi}{a}u\right)\\ &= \bar{\Phi}_\rho(2na+u).\end{aligned}$$

Thus, we obtain

$$\begin{aligned}\eta_1 &= -e^{ku}\sum_{j=0}^{\infty}{}' \frac{2}{a}\Re\left\{\int_{a}^{\infty} \bar{\Phi}_\rho(u)e^{i\frac{j\pi}{a}u}du\right\}\cos\left(\frac{j\pi}{a}u\right)\\ &= -e^{ku}\sum_{m=1}^{\infty}\left[\sum_{j=0}^{\infty}{}' \frac{2}{a}\Re\left\{\int_{ma}^{(m+1)a} \bar{\Phi}_\rho(u)e^{i\frac{j\pi}{a}u}du\right\}\cos\left(\frac{j\pi}{a}u\right)\right]\\ &= -e^{ku}\sum_{n=1}^{\infty}\left[\bar{\Phi}_\rho(2na-u)+\bar{\Phi}_\rho(2na+u)\right]\\ &= -\sum_{n=1}^{\infty} e^{-2akn}\left[\Phi_\rho(2na+u)+e^{2ku}\Phi_\rho(2na-u)\right],\end{aligned}$$

which completes the proof. □

The truncation error η_2 can be viewed as a summation in the tails of F_j's. Therefore, its bound should closely relate to the convergence rate of the sequence $\{F_j\}$, for which we need the following definition of algebraic convergence.

DEFINITION EC.1 (DEFINITION 2 IN SECTION 2.3 OF BOYD 2001). A sequence $\{a_i, i = 0,1,2,\ldots\}$ has an algebraic index of convergence s if s is the largest real number such that $\limsup_{i\to\infty} |a_i| i^s < \infty$.

We also need the following assumption to bound the error terms by the chosen parameters in the algorithm explicitly.

ASSUMPTION EC.1. *The algebraic index of convergence for the sequence:* $\left\{\Im\left\{[\mathcal{F}\bar{\Phi}'_\rho]\left(\frac{n\pi}{a}\right)\right\}\right\}_{n=0}^{\infty}$ *is some constant* $\beta > 0$.

REMARK EC.1. It is clear that $\bar{\Phi}_\rho(u)$ has an exponential decay at infinity, and so does its derivative $\bar{\Phi}'_\rho(u)$ in light of Karamata's theory (Boyd 2001). Assumption EC.1 states that the imaginary part of the Fourier transform of $\bar{\Phi}'_\rho(u)$ has a positive algebraic index of convergence. It is indeed a mild assumption, since there is good integrability in $\bar{\Phi}'_\rho(u)$ in light of the Riemann-Lebesgue lemma, such that a rate $\beta > 0$ can commonly be guaranteed.

PROPOSITION EC.5. *Let* C_k *be the constant such that* $\Phi_\rho(u) \le C_k e^{ku}$, *for all* $u \ge 0$. *Under Assumption EC.1, we have*

$$|\eta_1| \le C_k e^{-ka+2ku} \frac{\cosh ku}{\sinh ka}, \qquad |\eta_2| \le e^{ku} \frac{\beta C'_a}{J^\beta},$$

where $C'_a > 0$ *is a constant that only depends on* a.

Proof of Proposition EC.5. By Proposition EC.4, we know that

$$\begin{aligned}
|\eta_1| &= \left| \sum_{n=1}^{\infty} e^{-2akn} \left[\Phi_\rho(2na+u) + e^{2ku} \Phi_\rho(2na-u) \right] \right| \\
&\le \left| \sum_{n=1}^{\infty} e^{-2akn} \left[C_k e^{ku} + e^{2ku} C_k e^{ku} \right] \right| \\
&= C_k e^{-ka+2ku} \frac{\cosh ku}{\sinh ka}.
\end{aligned}$$

For the truncation error η_2, we first discuss the algebraic index of the sequence $\{F_n\}$. Through a simple application of integration by parts, we have

$$\begin{aligned} F_n &= \frac{2}{a}\Re\left\{\tilde{\bar{\Phi}}_\rho\left(i\frac{n\pi}{a}\right)\right\} = \frac{2}{a}\int_0^\infty \bar{\Phi}_\rho(z)\cos\left(\frac{n\pi}{a}z\right)dz \\ &= \frac{2}{n\pi}\int_0^\infty \bar{\Phi}_\rho(z)d\sin\left(\frac{n\pi}{a}z\right) = \frac{2}{n\pi}\Im\left\{\int_0^\infty \bar{\Phi}'_\rho(z)e^{i\frac{n\pi}{a}z}dz\right\}. \end{aligned}$$

Under Assumption EC.1, $\exists C'_a > 0$ and $N \in \mathbb{Z}^+$, such that $\forall n > N$, we have

$$\Im\left\{\int_0^\infty \bar{\Phi}'_\rho(z)e^{i\frac{n\pi}{a}z}dz\right\} \le \frac{C'_a}{n^\beta},$$

where C'_a is a constant that only depends on a. Consequently, we have a bound on the functions in the sequence; $F_n \le \frac{2C'_a}{\pi n^{1+\beta}}$. Therefore, the truncation error η_2 can be bounded by

$$\begin{aligned} |\eta_2| &= \left| e^{ku}\sum_{n=J+1}^{\infty} F_n\cos\left(\frac{n\pi}{a}u\right)\right| \\ &\le e^{ku}\sum_{n=J+1}^{\infty}|F_n| \\ &\le e^{ku}\frac{2\beta C'_a}{\pi J^\beta}. \end{aligned}$$

This completes the proof. □

Proposition EC.5 explicitly shows the relations between values of algorithm parameters and the resulting convergence errors. For any fixed pair of u and k, the absolute replacement error $|\eta_1|$ is of exponential decay in a. In practice, we choose a to be relatively larger than u to make the multiplier $\frac{\cosh ku}{\sinh ka}$ small enough. After determining a, the absolute truncation error $|\eta_2|$ converges to 0 with the convergence rate being the algebraic index of convergence β, as $J \to \infty$. To control the total error in a reasonably small range, we can first choose a large a to make η_1 small enough, and then set a proper J to adjust the truncation error.

EC.1.8. Supplementary Materials for Section 4.3

The Fourier-cosine method introduced in Section 4.2 calculates the value of the discounted cost objective for any given production rate ρ. As the next step, we only need to numerically search for

the minimizer of this one-variable function, which we can conveniently accomplish via some standard algorithms searching for the global minimum, including but not limited to, simulated annealing (Bertsimas and Tsitsiklis 1993), genetic algorithms (Forrest 1993), and interval-arithmetic-based techniques (Hansen and Walster 2003). In what follows, we apply a hybrid global optimization method proposed by Xu (2002), whose comparisons with the aforementioned classical methods are available in the first section of Xu (2002). Specifically, this method is deterministic without random sampling and is guaranteed to converge to the global optimal solution. As stated by Xu (2002), the idea has a relatively simple and intuitive analogy of climbing a mountain if we regard it as the maximization problem of the objective function $-\Phi_\rho(u)$. Whenever we climb to the summit of a mountain (local maximizer), we can check whether there is a higher mountain in the domain, move to the same level of the higher mountain, and then climb again. The process is repeated until we can no longer see any higher mountain when standing at the summit of the highest mountain (global maximizer). The interval Newton method achieves the checking and climbing procedures (Hansen and Walster 2003). Algorithm 1 gives the implementation details of searching for the optimal production rate based on the objective function calculated by the Fourier-cosine scheme. Theorem 1 in Xu (2002) indicates that the globally optimal solution is always warranted.

Algorithm 1 A hybrid global optimization algorithm (Xu 2002)

Input: initial inventory u, objective function $\Phi_\rho(u)$ for $\rho \geq 0$, where $\Phi_\rho(u)$ is evaluated by Fourier-cosine method using Equation (17) ($\xi > 0$);
Output: global minimum $(\rho^*, \Phi_{\rho^*}(u))$;
1: Initialize: Tol, u, $\rho^* = 0$, $\xi_{loc} = Tol$;
2: **repeat**
3: Set the domain $S = [\xi_{loc}, 1/Tol]$;
4: Find a local minimum $\Phi < \Phi_{\xi_{loc}}(u)$ in the domain and let $\xi^* \in S$ be the smallest root such that $\Phi_{\xi^*}(u) = \Phi$;
5: $\xi_{loc} = \xi^*$, $\rho^* = \frac{r + \Psi_D(\xi^*)}{\xi^*}$;
6: **until** No solution for $\Phi_\xi(u) = \Phi - \epsilon$ for $\xi \in [Tol, 1/Tol]$ can be found for the given error tolerance level Tol.

In the numerical experiments, we find that the cost objective function usually does not have many local minima, so we do not have to conduct the "searching and checking" procedure many times. Therefore, it is always very fast to establish the global minimum solution. For instance,

let us consider an example with compound Poisson demands following a mixture of Erlang size distributions where the Lévy measure is given by $\nu(dx)=\lambda\sum_{j=1}^{M}q_j\frac{\theta^j x^{j-1}e^{-\theta x}}{(j-1)!}dx$ for $x\geq 0$ and $\theta>0$. Specifically, λ is the Poisson intensity rate and $\{q_1,\ldots,q_M\}$ is a set of probabilities, i.e., $q_j\geq 0$ and $\sum_{j=1}^{M}q_j=1$. The mean of the Lévy measure is $\mu_\nu=\frac{1}{\lambda}\sum_{j=1}^{M}jq_j$, while its Laplace exponent is

$$\Psi_D(z)=\int_0^\infty\left(1-e^{-zx}\right)\nu(dx)=\lambda-\lambda\sum_{j=1}^{M}q_j\left(\frac{\theta}{\theta+z}\right)^j.$$

For convenience, we take $M=2$, $\{q_1,q_2\}=\{0.05,0.95\}$, $\theta=0.5$, $\lambda=10$, $u=1$, $h(x)=\sqrt{x}$, and $w(x)=K_2(1-e^{-\xi x})$ with $K_2=0.5$. Figure EC.1 plots $\Phi_{\rho(\zeta)}(u)$ against ζ. The minimum total cost $\Phi_{\rho^*(\zeta^*)}(u)$ is attained at $\zeta^*=0.0568$, or equivalently, $\rho^*=18.4750$, yielding $\Phi_{\rho^*(\zeta)}(u)=44.1550$. If we reset $K_2=0.3$ in the example above, we can get the corresponding plot in Figure EC.2. We observe that the local minimum is then $\Phi_{\hat{\rho}(\hat{\zeta})}(u)=35.9502$ at $\hat{\zeta}=0.1382$. However, it is clear from Figure EC.2 that as ζ goes to infinity, the total cost $\Phi_{\rho(\zeta)}(u)$ decreases to a limit that is smaller than this local minimum, i.e., $\lim_{\zeta\to+\infty}\Phi_{\rho(\zeta)}(u)<\Phi_{\hat{\rho}(\hat{\zeta})}(u)$. Specifically, Proposition 4 states that $\rho\to 0$ when $\zeta\to\infty$, and we can calculate that $\Phi_0(0)=K_2\lambda/r$ and

$$\tilde{\tilde{\Phi}}_0(z)=\frac{\tilde{\tilde{g}}(z)}{\Psi_D(z+k)+r}+\frac{K_2\lambda\Psi_D(z+k)}{r(z+k)(\Psi_D(z+k)+r)},\quad z\in\{a+bi:a\geq 0,b\in\mathbb{R}\}\backslash\{0,\zeta\}.$$

By applying our Fourier-cosine approximation (17), we compute $\Phi_0(u)=30.1441<35.9502$.

EC.2. Supplementary Materials for Section 5

EC.2.1. Assumptions of Theorem 3 and Related Discussions

As revealed by Lee et al. (2021), if one directly applies the Fourier-cosine method to approximate $f_t(x)$, the associated error terms when t is small could sometimes be divergent for some Lévy subordinators; for instance, this is the case for Gamma processes. Consequently, we first use the Fourier-cosine method to approximate a refined product $x^{n_0}f_t(x)$, where the presence of x^{n_0} helps to avoid the divergence in the Fourier-cosine approximation when t is near 0. After that, we divide the approximated value by x^{n_0} to recover $f_t(x)$. Accordingly, the Fourier transform of $x^{n_0}f_t(x)$ is given by

$$[\mathcal{F}(x^{n_0}f_t(x))](s)=(-i)^{n_0}\frac{d^{n_0}}{ds^{n_0}}[\mathcal{F}f_t](s).$$

Figure EC.1 The discounted cost $\Phi_{\rho(\zeta)}(u)$ for a compound Poisson demand with a mixture of Erlangs ($K_2 = 0.5$).

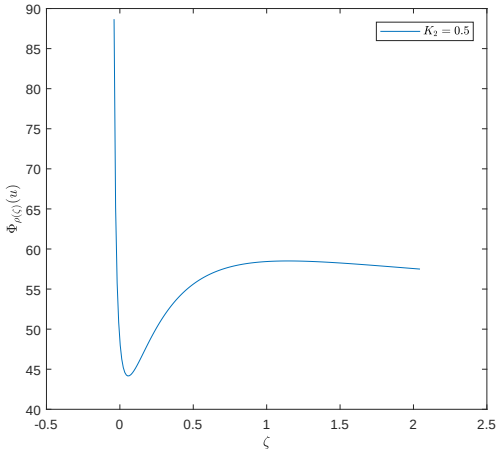

Figure EC.2 The discounted cost $\Phi_{\rho(\zeta)}(u)$ for a compound Poisson process with a mixture of Erlangs ($K_2 = 0.3$).

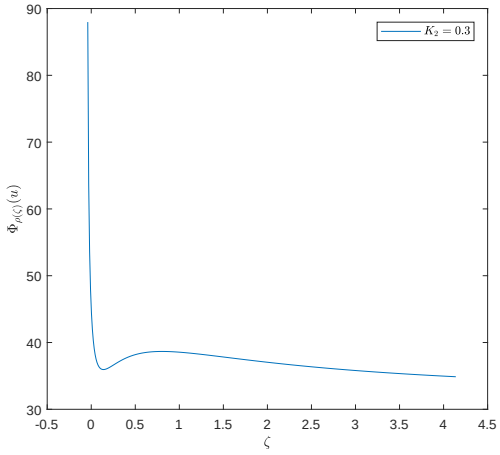

Before proving Theorem 3, we first state the following two technical assumptions; see Lee et al. (2021) for additional details.

ASSUMPTION EC.2. *There exists a positive integer n_0 such that*

i) $|\Psi_D^{(1)}(s)| = O\left(s^{-\frac{1+\theta}{n_0}}\right)$ *and* $|\Psi_D^{(n_0)}(s)| = O\left(s^{-(1+\theta)}\right)$ *hold for some* $\theta > 0$*;*

ii) if $n_0 \geq 2$*, for all* $m = 2, \cdots, n_0$*, both* $x^m\pi(x)$ *and* $x^m\pi'(x)$ *are integrable, i.e.,* $x^m\pi(x), x^m\pi'(x) \in L^1(\mathbb{R}^+)$*, where* $\pi(x)$ *is the density function of the Lévy measure, i.e.,* $\nu(dx) = \pi(x)dx$*, with a derivative* $\pi'(x)$*.*

REMARK EC.2. As an illustrative example, if the reserve process $R(t)$ is a compound Poisson process with a Poisson arrival intensity λ and demand size distribution Gamma(α, β), the corresponding density function is $\pi(x) = \frac{\lambda\beta^\alpha}{\Gamma(\alpha)}x^{\alpha-1}e^{-\beta x}$ for $x > 0$, and the Laplace exponent is $\Psi_D(s) = \lambda(1 + \frac{s}{\beta})^{-\alpha} - \lambda$. We can easily check that Assumption EC.2 is satisfied if we let $n_0 = 1$. For other cases, especially for frequently used demand processes, the parameter n_0 can be similarly determined via checking the convergence order of $\Psi_D^m(s)$ in s.

ASSUMPTION EC.3. *The density function $f_t(x)$ is jointly continuous for $(x,t) \in \mathbb{R}^+ \times (0,T]$, and there exists an $x_0 > 0$ such that $f_t'(x) < 0$ for $(x,t) \in (x_0, \infty) \times (0,T]$.*

REMARK EC.3. A smoothness condition on the density function f_t is naturally required for evaluating an integral expression involving f_t.

EC.2.2. Proof of Theorem 3

We first prove the representation (22) for the finite-time stockout probability $\phi_u(T)$. For convenience, we adjust the time scale using the multiplier ρ to define $\hat{R}(\rho t) := R(t)$ and $\hat{D}(\rho t) := D(t)$. We thus obtain

$$\hat{R}(t) = R(t/\rho) = u + t - D(t/\rho) = u + t - \hat{D}(t).$$

In this way, the production rate is standardized as 1, and $\hat{D}(t)$ is still a Lévy subordinator with the Lévy measure being $\hat{\nu}(dx) = \nu(dx)/\rho$. Correspondingly, we further have

$$\hat{\tau}_u := \inf\{t > 0 : \hat{R}(t) < 0\} = \inf\{t > 0 : R(t/\rho) < 0\} = \rho \inf\{t > 0 : R(t) < 0\} = \rho\tau_u.$$

By respectively setting the initial surplus as u and the time parameter as ρT in the finite-time ruin probability formula given by Equation (4.1) in Lee et al. (2021), we can obtain

$$\begin{aligned}
&\phi_u(T) = \mathbb{P}(\tau_u < T) = \mathbb{P}(\hat{\tau}_u < \rho T) = 1 - \mathbb{P}(\hat{\tau}_u \geq \rho T) \\
=&1 - \mathbb{P}(\hat{D}(\rho T) = 0) - \int_0^{u+\rho T} \hat{f}_{\rho T}(z)dz + \int_0^{\rho T} \left[1 - \frac{1}{z}\int_0^z \hat{S}_z(x)dx\right] \hat{f}_{\rho T - z}(u + \rho T - z)dz \\
=&1 - \mathbb{P}(D(T) = 0) - \int_0^{u+\rho T} f_T(z)dz + \int_0^{\rho T} \left[1 - \frac{1}{z}\int_0^z S_{z/\rho}(x)dx\right] f_{T - z/\rho}(u + \rho T - z)dz \\
=&1 - \mathbb{P}(D(T) = 0) - \int_0^{u+\rho T} f_T(z)dz + \rho \int_0^{T} \left[1 - \frac{1}{\rho z}\int_0^{\rho z} S_z(x)dx\right] f_{T - z}(u + \rho(T - z))dz,
\end{aligned}$$

where $\hat{f}_t$ and $\hat{S}_t$ are the respective density and survival functions of $\hat{D}_t$, with the identities $\hat{f}_t = f_{t/\rho}$ and $\hat{S}_t = S_{t/\rho}$.

Next, we show that the error in approximating the finite-time stockout probability $\phi_u(T)$ by (25) can be made arbitrarily small. This part can be analogously established using the proof similar to that of Theorem 4.1 in Lee et al. (2021). Therefore, we only outline the main steps to make the presentation self-contained; see Lee et al. (2021) for details.

The numerical errors are incurred in approximating two separate integrals in (22). First, applying the Fourier-cosine method described in Section 4.2, the term $\int_0^{u+\rho T} f_T(z)dz$ in (22) can be approximated by $\sum_{j=0}^{J}{}' F_j^{(1)}(T)\chi_j(u-d+\rho T)$. Moreover, we can obtain bounds on the corresponding approximation error terms ε_1 and ε_2 as below:

$$|\varepsilon_1| := \left| -\frac{2}{a}\sum_{j=0}^{J}{}' \chi_j(u-d+\rho T)\int_a^{\infty} f_T(x)\cos\left(\frac{j\pi}{a}x\right)\mathrm{d}x \right| \le \left| 1+\frac{2}{\pi}\int_0^{\pi}\frac{\sin z}{z}\mathrm{d}z \right| S_T(a),$$

$$|\varepsilon_2| := \left| \sum_{j=J+1}^{\infty}{}' \chi_j(u-d+\rho T)F_j^{(1)}(T) \right| \le \frac{C'_a}{J^{\beta}},$$

where the first inequality follows from a delicate analysis on the well-known series in Gibbs phenomenon, i.e., $S_n(x) := \sum_{k=1}^{n}\frac{\sin(kx)}{k}$, and some useful properties of $S_n(x)$ can be found in Hewitt and Hewitt (1979). The detailed derivation is given in Lemma D.1 in the supplementary material to Lee et al. (2021). Clearly, the approximation error $\mathcal{E}$ can be made arbitrarily small by choosing large enough a and J, which are truncation parameters in the Fourier-cosine algorithm.

Second, the integrand terms $A(z) := 1-\frac{1}{\rho z}\int_0^{\rho z} S_z(x)dx$ and $B(z) := f_{T-z}(u+\rho(T-z))$ in (22) can also be approximated by following the same vein using $\hat{A}(z) := 1-\frac{1}{\rho z}\sum_{j=0}^{J}{}' F_j^{(2)}(z)\chi_j(\rho z)$ and $\hat{B}(z) := \frac{\sum_{j=0}^{J}{}' F_j^{(3)}(T-z)\cos\frac{j\pi(u+\rho(T-z))}{a}}{(u+\rho(T-z))^{n_0}}$, respectively. Again, by choosing a suitably large enough a and J, both approximation errors $|A(z)-\hat{A}(z)|$ and $|B(z)-\hat{B}(z)|$ can be made arbitrarily small, holding uniformly over $z\in(0,T)$ (see Lemmas D.2 and D.3 in the supplementary material of Lee et al. 2021). To finish the proof, we only need to show that the approximation error for $\int_0^T A(z)B(z)\mathrm{d}z$ can be made arbitrarily small by choosing suitably large a and J. Notice that

$$\begin{aligned}
&\left|\int_0^T A(z)B(z)\mathrm{d}z - \int_0^T \hat{A}(z)\hat{B}(z)\mathrm{d}z\right| \\
\le&\int_0^T |A(z)||B(z)-\hat{B}(z)|\mathrm{d}z + \int_0^T |A(z)-\hat{A}(z)||B(z)|\mathrm{d}z + \int_0^T |A(z)-\hat{A}(z)||B(z)-\hat{B}(z)|\mathrm{d}z \\
\le& T\cdot\left[\sup_{z\in[0,T]}|A(z)|\cdot\sup_{z\in[0,T]}|B(z)-\hat{B}(z)| + \sup_{z\in[0,T]}|B(z)|\cdot\sup_{z\in[0,T]}|A(z)-\hat{A}(z)|\right] \\
&+T\cdot\sup_{z\in[0,T]}|A(z)-\hat{A}(z)|\cdot\sup_{z\in[0,T]}|B(z)-\hat{B}(z)|.
\end{aligned}$$

It then remains to show that $\sup_{z\in[0,T]}|A(z)|$ and $\sup_{z\in[0,T]}|B(z)|$ are both finite, which is equivalent to proving that $\frac{1}{\rho z}\int_0^{\rho z} S_z(x)dx$ and $f_{T-z}(u+\rho(T-z))$ are both uniformly bounded over $z\in(0,T)$.

The uniform boundedness of $\frac{1}{\rho z}\int_0^{\rho z} S_z(x)dx$ is relatively straightforward, which follows from the fact that

$$\frac{1}{\rho z}\int_0^{\rho z} S_z(x)dx \le \frac{1}{\rho z}\int_0^{\infty} S_z(x)dx = \frac{\mu_\nu}{\rho}.$$

As for $f_{T-z}(u+\rho(T-z))$, we recall the joint continuity of $f_t(x)$ in $(x,t)\in\mathbb{R}\times(0,T]$ under Assumption EC.3, indicating that $f_{T-z}(u+\rho(T-z))$ is continuous in $z\in[0,T)$. Consequently, we have $\lim_{z\to 0+} f_z(u+\rho z)=0$ for $u>0$, and then $\sup_{z\in[0,T)} f_{T-z}(u+\rho(T-z))<\infty$, which completes the proof.

□

EC.2.3. Proof of Proposition 5

By the monotone convergence theorem, we know

$$\varphi(u)=\mathbb{E}[\tau_1|I(0)=u]=-\lim_{r\to 0^+}\frac{d}{dr}\mathbb{E}\left[e^{-r\tau_1}\middle|I(0)=u\right]=-\lim_{r\to 0^+}\frac{d}{dr}d_{r,\rho}(u).$$

Taking the Laplace transform in u on both sides gives

$$\tilde{\varphi}(u)=-\lim_{r\to 0^+}\frac{d}{dr}\tilde{d}_{r,\rho}(u).$$

We can derive the desired result using the Laplace transform of $d_{r,\rho}(u)$ given in Proposition EC.3.

□

EC.2.4. Proof of Theorem 4

By applying our Fourier-cosine scheme (17) on $\varphi(u)$ with the Laplace transform given in Proposition 5, we obtain

$$\varphi(u)=e^{ku}{\sum_{j=0}^{J}}' F_j^{(5)}\cos\left(\frac{j\pi}{a}u\right)+\varepsilon_1+\varepsilon_2,$$

where $F_j^{(5)}=\frac{2}{a}\Re\left\{\tilde{\varphi}\left(k-i\frac{j\pi}{a}\right)\right\}$, the replacement error ε_1 is

$$\varepsilon_1=-e^{ku}{\sum_{j=0}^{\infty}}'\frac{2}{a}\Re\left\{\int_a^{\infty}e^{-ku}\varphi(u)e^{i\frac{j\pi}{a}u}du\right\}\cos\left(\frac{j\pi}{a}u\right),$$

and the truncation error ε_2 is

$$\varepsilon_2=e^{ku}\sum_{j=J+1}^{\infty}F_j^{(5)}\cos\left(\frac{j\pi}{a}u\right).$$

Let C_k be the constant such that $\varphi(u) \le C_k e^{ku}$ for all $u \ge 0$, and $\beta > 0$ be the algebraic index of convergence for the sequence $\left\{\Im\left\{[\mathcal{F}\bar{\varphi}']\left(\frac{n\pi}{a}\right)\right\}, n = 0, 1, 2, \ldots\right\}$. By Proposition EC.5, we have

$$|\varepsilon_1| \le C_k e^{-ka+2ku} \frac{\cosh ku}{\sinh ka}, \qquad |\varepsilon_2| \le e^{ku} \frac{\beta C'_a}{J^\beta},$$

where $C'_a > 0$ is a constant that depends only on a. Therefore, for any $\epsilon > 0$ and a fixed $k > 0$ and $u > 0$, there exist large enough $a > 0$ and $J > 0$, such that

$$|\varepsilon_1| \le C_k e^{-ka+2ku} \frac{\cosh ku}{\sinh ka} < \frac{\epsilon}{2}, \qquad |\varepsilon_2| \le e^{ku} \frac{\beta C'_a}{J^\beta} < \frac{\epsilon}{2}.$$

The total approximation error is thus less than ϵ, and we complete the proof. □

EC.2.5. Proof of Proposition 6

We observe that $\mathcal{L}_\tau(u) := \mathbb{E}[L(\tau_1)|I(0) = u]$ is a special case of $c_{r,\rho}(u)$ by letting $h(x) \equiv 0$, $w(x) = x$, and $r = 0$. Thus, substituting these expressions into Proposition 1, we can obtain the desired Laplace transform of $\mathcal{L}_\tau(u)$. □

EC.2.6. Proof of Theorem 5

Replacing $\varphi(u)$ in the proof of Theorem 4 with the target function $\mathcal{L}_\tau(u)$ and based on the Laplace transform of $\mathcal{L}_\tau(u)$ in Proposition 6, we can use a similar argument to establish the approximation error bound for $\mathcal{L}_\tau(u)$ as follows,

$$|\varepsilon_1| \le C_k e^{-ka+2ku} \frac{\cosh ku}{\sinh ka}, \qquad |\varepsilon_2| \le e^{ku} \frac{\beta C'_a}{J^\beta},$$

where the constant C_k and index β depend on the properties of the target function $\mathcal{L}_\tau(u)$. For any $\epsilon > 0$ and a fixed $k > 0$ and $u > 0$, we can then choose large enough $a > 0$ and $J > 0$ such that $|\varepsilon_1| < \frac{\epsilon}{2}, |\varepsilon_2| < \frac{\epsilon}{2}$, which completes the proof. □

EC.2.7. Proof of Proposition 7

Notice that after the first stockout, the inventory process renews from $u = 0$ and repeats the same renewal cycle. Therefore, the long-run stockout occurrence rate is time-consistent in that it is

independent of the initial inventory level u, provided that $\mathbb{E}[\tau_1] < \infty$, which is guaranteed under the stability condition $\rho < \mu_\nu$. Let the inter-arrival times of the demand process be denoted by $T_1, T_2, \cdots$, which are i.i.d. exponentially distributed random variables given that the demand $D(t)$ is a compound Poisson process. By Theorem 3.4.4 in Ross et al. (1996), we have

$$\pi = \mathbb{E}\left[\frac{T_{N_A(\tau_1)}}{\tau_1}\middle| I(0)=0\right] = \frac{\mathbb{E}[T_1]}{\mathbb{E}[\tau_1|I(0)=0]} = \frac{1}{\lambda\varphi(0)}. \qquad \square$$

EC.2.8. Proof of Proposition 8

By setting the initial inventory level to 0 ($u=0$), the inventory process can be regarded as a renewal process that starts from zero inventory at time $t=0$ and renews with zero inventory at time τ_1. Thus, the sequence $\{(\tau_1, L(\tau_1)), (\tau_2-\tau_1, L(\tau_2)-L(\tau_1)), \ldots\}$ is independent and identically distributed. Consider an alternative renewal process that is initially at the status "on" until the time $\rho\tau_1$ and then takes "off" status until $\rho\tau_1 + L(\tau_1)$ in the first period. Then the "off" state in the first period lasts for $L(\tau_1)$, and the duration of the first period is $\rho\tau_1 + L(\tau_1) = D(\tau_1)$. By the renewal theorem, i.e., Theorem 3.4.4 in Ross et al. (1996), we immediately have

$$l = \mathbb{P}(\text{the system is off}) = \lim_{t\to\infty}\mathbb{E}\left[\frac{L(t)}{D(t)}\right] = \frac{\mathbb{E}[L(\tau_1)]}{\mathbb{E}[D(\tau_1)]} = \frac{\mathcal{L}_\tau(0)}{\mu_\nu\varphi(0)}. \quad \square$$

EC.2.9. Proof of Proposition 9

Given the probability space $(\Omega, \mathcal{F}, \mathbb{P})$, for any fixed $\omega \in \Omega$, let $\{D(t,\omega), t \geq 0\}$ be the sample path of the demand process. For any two production rates $0 < \rho_1 < \rho_2$, we denote $I_i(t)$ and A_i as the corresponding inventory process and the event $\{\tau_u < T\}$ under these two replenishment rates ρ_i, $i = 1, 2$. By the definition of stockout probability $\phi_u(T) := \mathbb{P}(\tau_u < T)$, to prove that $\phi_u(T)$ is non-increasing in ρ, it is equivalent to verify $\mathbb{P}(A_1) \geq \mathbb{P}(A_2)$. We then only need to show that for any fixed $\omega \in A_2$, i.e., the sample path $\{I_2(t,\omega), t \geq 0\}$ leads to a finite-time stockout event A_2, the corresponding sample path $\{I_1(t,\omega), t \geq 0\}$ under the same sample scenario ω must incur the occurrence of A_1, that is $\omega \in A_1$. Clearly, since $\rho_1 < \rho_2$, we have $I_1(t,\omega) < I_2(t,\omega)$. Therefore, the occurrence of A_2 implies that of A_1, and hence $\phi_u(T)$ is decreasing in ρ.

For other quantities, one can re-define the events $\{A_i, i = 1, 2\}$ accordingly to the particular context, and similar arguments are also valid to obtain their comparative statics in the production rate ρ. $\square$

EC.3. Numerical Experiments I: System Costs and Optimal Production Rates

In this section, we provide supplementary details on the numerical experiments in Section 6. In Section EC.3.1, we discuss the appropriate choices of the numerical parameters in the Fourier-cosine method that would yield high accuracy of approximations. In Section EC.3.2, we apply the Fourier-cosine method to numerically compute the optimal replenishment rates and the associated costs under different Lévy demands. The robustness of the numerical approximations is also examined. These results echo the versatility and effectiveness of our framework. In addition, we combine the unaccelerated Fourier-cosine scheme with several popular filters to reduce commonly observed oscillations and compare their performance in Section EC.3.3. Finally, we compare our Fourier-cosine method with the celebrated Talbot numerical scheme (Abate and Whitt 2006) in Section EC.3.4.

EC.3.1. Appropriate Choices of Numerical Parameters

Notice that there are altogether three parameters to settle in our Fourier-cosine scheme, i.e., the dampening parameter k, the truncation parameters of the domain a, and the truncation index of the summation series J. Before presenting the numerical experiments, we separately discuss their effects on the results and give several recommendations for choosing their values.

First, for the dampening parameter k, we highlight an implicit requirement that it should keep $\zeta = \xi - k$ strictly positive as stated in Proposition 4. While a larger k may help reduce the *replacement error* η_1 given in (18), it must be strictly smaller than the positive root of the Lundberg equation, requiring an initial guess on ξ. However, the Lundberg equation depends on the replenishment rate, whose optimal value is not known a priori. We can thus first derive ξ^* using Algorithm 1 with a given value of k, say $k = 0.1$, and then repeat Algorithm 1 for a reasonable choice of $k^* < \xi^*$.

In fact, the numerical results are pretty robust in different choices of k, which we will illustrate later.

Next, since the truncation parameters a and J are directly involved in the error terms η_1 and η_2, the trade-off between computational precision and efforts should be carefully balanced when choosing their values. As shown in the error analysis in Section EC.1.7, for any given error tolerance level ϵ, a large enough a can well control the *replacement error* such that $\eta_1 < \epsilon/2$, while a proper J can manage the *truncation error* so that $\eta_2 < \epsilon/2$. Particularly with a fixed a, the *truncation error* η_2 converges to 0 when J increases to infinity, and the lower error bound thus becomes η_1. However, a larger value of a shall increase the *truncation error* η_2, and a larger J is then needed to maintain the same precision level. For practical applications, we do not associate the value of a to a specified error ϵ, which could be rather complicated. Instead, we here propose a rule-of-thumb choice for a. Since it is reasonable to assume that the cost functions $h(\cdot)$ and $w(\cdot)$ have at most algebraic growths, so does $\Phi_\rho(u)$ and the decay rate of $\bar{\Phi}_\rho(u) = e^{-ku}\Phi_\rho(u)$ is generally governed by the factor e^{-ku}. We aim to make $e^{-ka}\Phi_\rho(a)$ small enough and let $e^{-ka} < 10^{-m}$, which leads to $a > \ln(10^m)/k$, for some $m = 1, 2, \ldots$. Taking the initial inventory level u and the loading factor μ_v into consideration and setting $m = 4$, we have the following recommendation for choosing a that only depends on k:

$$a = u + \mu_\nu + \frac{\ln(10^4)}{k}. \tag{EC.40}$$

As shown later, this recommended choice works well in all numerical experiments. As for the other truncation parameter J, once we have determined k and a, we can choose a large enough J to attain high precision while the computational complexity remains linear in J. In what follows, we follow the suggestions of Li et al. (2021) to set it as $J = 2^9$.

EC.3.2. Optimal Replenishment Rate under Various Model Settings

In this section, we find the optimal replenishment rates and associated costs where the demand dynamics has either a finite Lévy measure, such as a compound Poisson process, or an infinite Lévy

measure, such as a Gamma process and an inverse Gaussian process. In practice, the Gamma and inverse Gaussian processes are commonly adopted in describing one-directional stochastic dynamics such as the degradation modeling in system maintenance (Van Foreest and Wijngaard 2014) and the claim process in insurance (Asmussen and Albrecher 2010). Specifically, we consider different combinations of cost functions for each case. In all cases, we demonstrate that our Fourier-cosine method provides a robust and efficient means to compute the optimal replenishment rates and associated costs. We take the discount rate $r = 0.1$. For other interest rate choices, the effectiveness of our proposed Fourier-cosine method can also be clearly seen.

EC.3.2.1. Finite Lévy Measure Cases The most typical example of the Lévy subordinator with finite Lévy measure is the compound Poisson process. We assume an exponentially distributed demand size and simple cost functions such as linear ones, where closed-form solutions for the cost objective $\Phi_\rho(0)$ and the corresponding optimal replenishment rate are available. When $u > 0$, we have no closed-form solutions and resort to our Fourier-cosine method.

Example EC.1 (compound Poisson process with exponential demands). Consider the case when the Lévy subordinator is a compound Poisson process with an exponentially distributed demand size. The Lévy measure is $\nu(dx) = \lambda\mu e^{-\mu x}dx$, where λ is the Poisson intensity and μ is the rate of the exponential distribution. The expectation of the Lévy measure is then $\mu_\nu = \lambda/\mu$. Accordingly, the Laplace exponent becomes $\Psi_D(z) = \frac{\lambda z}{\mu+z}$. Moreover, we assume simple cost functions where the holding cost function is $h(x) = x$ and the lost-sales penalty is $w(x) = 100$, from which we can compute $\tilde{\bar{g}}(z)$ using (EC.36). In this case, the closed-form solution for minimizing $\Phi_\zeta(0)$ for ζ is available in Shi et al. (2014). The Poisson intensity λ is set to 1, and we use the Newton method with a tolerance error level of 10^{-5} to find the minimum $\Phi_\zeta(0)$ in Algorithm 1. Table EC.1 illustrates the results, and we observe that the optimal replenishment rate ρ^* increases with larger μ_ν. Thus, a larger replenishment rate should be set to satisfy the stronger demand and avoid losses due to lost sales. We also notice that the optimal average cost $F_{\rho_0^*}$ is $r\Phi_{\rho^*}(0)$, and the corresponding optimal replenishment rate ρ_0^* under the average cost criterion can also be easily calculated, as illustrated in Table EC.1.

Table EC.1 Optimal rates for $\Phi_\rho(0)$ and F_ρ under compound Poisson demands with exponential sizes for different μ_ν

μ_ν	0.05	0.1	0.5	1	5	10	20
ρ^*	0.2675	0.4031	1.1218	1.8000	5.6180	9.0000	13.528
ρ_0^*	0.0489	0.0968	0.4646	0.9000	3.8820	6.8377	11.0557
$\Phi_{\rho^*}(0)$	44.221	62.246	136.42	190.00	397.21	532.46	694.43
$F_{\rho_0^*}$	4.422	6.225	13.642	19.000	39.721	53.246	69.443

With the same setting, we also provide the corresponding results with different positive initial inventory levels in Table EC.2 when $\mu_\nu = 2$ and Table EC.3 when $\mu_\nu = 20$, respectively. Closed-form solutions are no longer available, and we use the approximated values obtained by Shi et al. (2014) as a benchmark. Both Tables EC.2 and EC.3 indicate that the optimal replenishment rate ρ^* decreases with higher initial inventory u. It is reasonable since the holding cost associated with a high inventory level is already high, and the latter could also be enough to serve the arriving demands; the firm then needs to reduce production to release the mounting pressure from the unsold inventory. However, the minimum total cost is not monotone in u. Instead, it is minimized at u being around 10 and 25, for $\mu_\nu = 2$ and $\mu_\nu = 20$, respectively. Moreover, $\min_u \Phi_\rho(u)$ is smaller for a smaller μ_ν because greater demand may induce a significant amount of lost-sales penalties. Meanwhile, we plot, for a fixed initial level u, $\Phi_{\rho^*}(u)$ against a in Figure EC.3 to illustrate the robustness of the approximation in a. Our recommended choices of a introduced in Section EC.3.1 are also indicated. The approximation is very close to the reference value and becomes stable when a exceeds 150.

EC.3.2.2. Infinite Lévy Measure Cases The Lévy subordinator with an infinite Lévy measure can be used to model a large number of sales with a relatively heavy-tailed size distribution (D'Auria and Samorodnitsky 2005). In this respect, we now consider Gamma and inverse Gaussian processes as the demand dynamics and illustrate the corresponding numerical results.

Example EC.2 (Gamma process). We assume that the Lévy subordinator is a Gamma process with the Lévy measure being $\nu(dx) = (\alpha e^{-\beta x}/x)\,dx$ for $x > 0$, and $\alpha, \beta > 0$. Consequently, the mean

Table EC.2 Optimal $\Phi_\rho(u)$ and ρ for compound Poisson demands with exponential sizes, where $\lambda=1$, $\mu_\nu=2$, and $k=0.05$.

u	5	10	15	20	25	30	40	50
ρ^*	2.5101	2.1700	1.8943	1.6582	1.4465	1.2503	0.8854	0.5411
Ref.	2.515	2.171	1.893	1.660	1.447	1.250	0.885	0.541
$\Phi_{\rho^*}(u)$	193.4488	181.4906	191.8075	212.6420	239.1562	269.0391	334.5168	404.1479
Ref.	193.450	181.490	191.810	212.640	239.160	269.040	334.520	404.150

Table EC.3 Optimal $\Phi_\rho(u)$ and ρ for compound Poisson demands with exponential sizes, where $\lambda=1$, $\mu_\nu=20$, and $k=0.03$

u	5	10	15	20	25	30	40	50
ρ^*	13.3480	13.1465	12.9259	12.6886	12.4365	12.1715	11.6081	11.0080
Ref.	13.356	13.147	12.928	12.685	12.437	12.171	11.609	11.007
$\Phi_{\rho^*}(u)$	684.4248	676.9089	671.6808	668.5787	667.4442	668.1301	674.4260	686.4918
Ref.	684.430	676.910	671.680	668.580	667.440	668.130	674.430	686.490

Figure EC.3 The discounted cost $\Phi^*_\rho(u)$ for a compound Poisson process in Example EC.1 with $\mu_\nu=2$, $u=10$, and $k=0.05$.

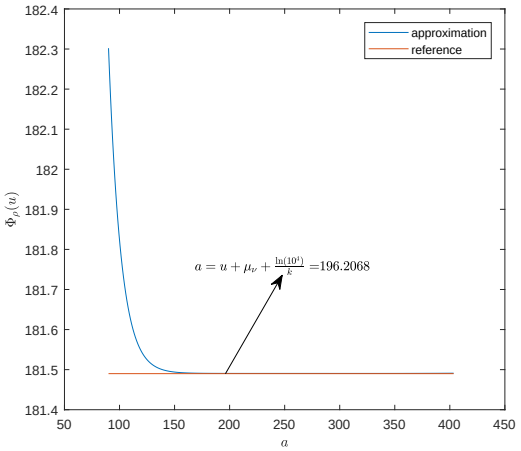

Figure EC.4 The discounted cost $\Phi_{\rho^*}(u)$ for a Gamma process in Example EC.2 when $u=10$.

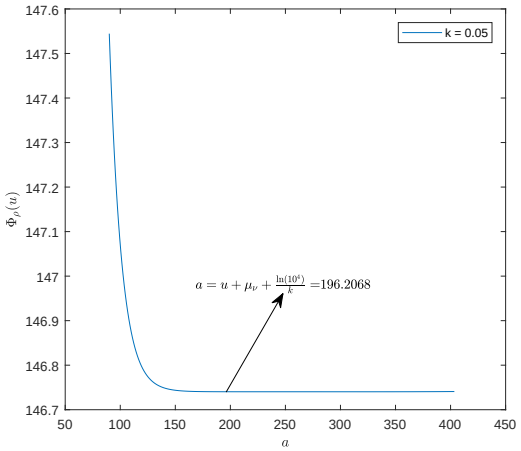

is now $\mu_\nu=\alpha/\beta$. At any fixed time $t>0$, the subordinator follows a Gamma distribution $\Gamma(\alpha t,\beta)$. The Laplace exponent then becomes $\Psi_D(z)=\alpha\ln\left(\frac{z+\beta}{\beta}\right)$. We respectively set the holding cost and the lost-sales penalty function as $h(x)=x$ and $w(x)=50x$, from which $\tilde{\bar{g}}(z)$ can be obtained by

(EC.37). Algorithm 1 is then adopted to find the optimal ζ^* in minimizing $\Phi_\zeta(u)$. The tolerance error level is again set at 10^{-5}. Table EC.4 presents the optimal ρ^* and $\Phi_{\rho^*}(u)$ for different values of u when $\mu_\nu = 2$. The other parameter settings are also specified there. No closed-form or reference solutions are available, and, to the best of our knowledge, ours is the first study on the production-inventory system under a Gamma demand process. The Gamma demand in this example is also different from that in Shi et al. (2014) in that they use the compound Poisson framework with the demand size following a Gamma distribution.

A similar phenomenon as in Example EC.1 can be observed. The optimal replenishment rate ρ^* decreases when the initial inventory u increases, and the optimal total cost $\Phi_{\rho^*}(u)$ is minimized when the initial inventory u is around 10. We also study the robustness of the optimal $\Phi_{\rho^*}(u)$, again for a fixed u, with respect to a in Figure EC.4 for $k = 0.05$. Our suggested choice of a also works well in this example. The approximation arrives at a stable convergence when a exceeds 150. Moreover, we also illustrate the optimal replenishment rates with different values of μ_ν under the average cost criterion in Table EC.5.

Table EC.4 Optimal ρ^* and $\Phi_{\rho^*}(u)$ with Gamma demands. Other parameters are $\alpha = 0.8$, $\mu_\nu = 2$, and $k = 0.05$.

u	5	10	15	20	25	30	40	50
ρ^*	2.3184	2.0099	1.7646	1.5532	1.3607	1.1797	0.8370	0.5088
$\Phi_{\rho^*}(u)$	147.6205	146.7404	164.6046	190.6999	221.0270	253.7716	323.2214	395.4711

Table EC.5 Optimal ρ_0^* and $F_{\rho_0^*}$ under the average cost criterion with Gamma demands.

μ_ν	0.05	0.1	0.5	1	5	10	20
ρ_0^*	0.0444	0.0888	0.4442	0.8884	4.4418	8.8836	17.7672
$F_{\rho_0^*}$	0.5182	1.0363	5.1815	10.3630	51.8150	103.6300	207.2601

Example EC.3 (Inverse Gaussian process). We consider the case when the Lévy subordinator is an inverse Gaussian process with the Lévy measure $\nu(dx) = \frac{\delta}{\sqrt{2\pi x^3}} e^{-\frac{\gamma^2 x}{2}} dx$ for $x > 0$ and its mean becomes $\mu_\nu = \frac{\delta}{\gamma}$. An inverse Gaussian process means that the process at time 1 follows an inverse Gaussian distribution $IG(\delta, \gamma)$. Similar to the Gamma process, its additivity property implies that at time t, the process is also inversely Gaussian distributed with the parameters being

$t\delta$ and γ. The corresponding Laplace exponent is $\Psi_D(z)=\delta(\sqrt{\gamma^2+2z}-\gamma)$. We assume fully non-linear cost functions here, where $h(x)=\sqrt{x}$ and $w(x)=5(1-e^{-x})$. Therefore, $\tilde{\tilde{g}}(z)$ can be obtained by (EC.39) and (EC.38). In this numerical experiment, we further set $\delta=1$, $\gamma=1/2$, and the tolerance error level as 10^{-5}. The optimal ρ^* and $\Phi_{\rho^*}(u)$ for different values of u are presented in Table EC.6 when $\mu_\nu=2$. Although no reference solutions are valid, the convergence shows to be stable and fast. We respectively plot the optimal $\Phi_{\rho^*}(u)$ in terms of the parameter a in Figure EC.5 for $k=0.05$ and in Figure EC.6 for $k=0.1$. These two plots show that a larger k needs a smaller a to reach a stable convergence. Our recommended choice of a fits well again in the convergence region. The optimal rates corresponding to the average cost are presented in Table EC.7.

Table EC.6 Optimal ρ^* and $\Phi_{\rho^*}(u)$ for an inverse Gaussian demand with $\delta=1$, $\mu_\nu=2$, and $k=0.05$.

u	5	10	15	20	25	30	40	50
ρ^*	2.4906	2.1967	1.9858	1.8175	1.6757	1.5523	1.3433	1.1692
$\Phi_{\rho^*}(u)$	41.2906	41.8567	44.0760	46.9487	50.0964	53.3432	59.8226	66.0785

Table EC.7 Optimal ρ_0^* and $F_{\rho_0^*}$ under the average cost criterion for an inverse Gaussian demand.

μ_ν	0.05	0.1	0.5	1	5	10	20
ρ_0^*	0.0499	0.0997	0.4874	0.9349	2.9425	3.7206	4.2013
$F_{\rho_0^*}$	1.3831	1.7405	2.9071	3.5113	4.7712	5.1190	5.3286

Figure EC.5 The discounted cost $\Phi_{\rho^*}(u)$ for an inverse Gaussian demand with $k=0.05$.

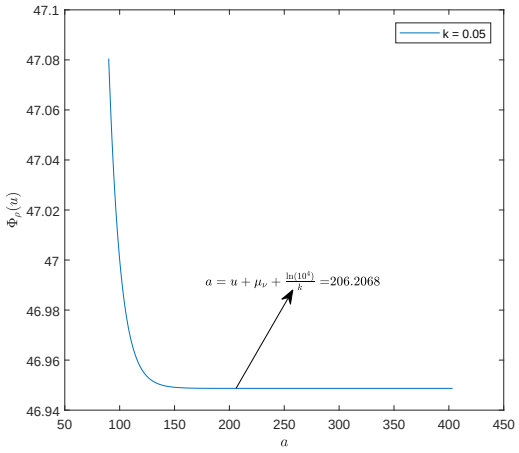

Figure EC.6 The discounted cost $\Phi_{\rho^*}(u)$ for an inverse Gaussian demand with $k=0.1$.

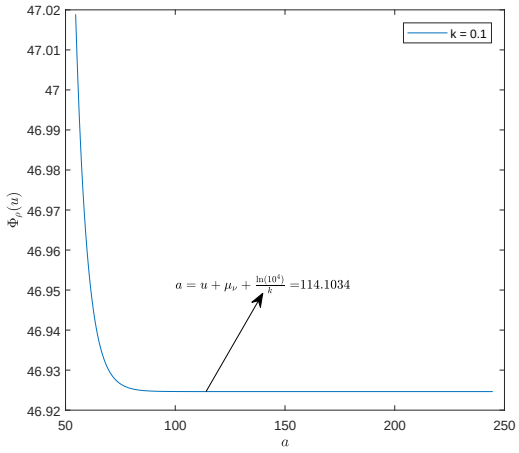

EC.3.2.3. Influence of Different Dynamics on the Optimal Rate In practice, the demand dynamics could be quite different depending on the nature of the business and products, and our general Lévy framework offers a high degree of modeling flexibility. In this section, we investigate the impact of the demand dynamics on optimal replenishment rates. Specifically, we consider the following five different demands with the same mean $\mu_\nu = 20$. The holding cost and lost-sales penalty are assumed to be $h(x) = x$ and $w(x) = 100$, respectively.

Setting I : A compound Poisson process with exponential demands as specified in Example EC.1 and the corresponding Lévy measure is $\nu(dx) = \lambda\mu e^{-\mu x}dx$, where $\lambda = 1$ and $\mu = 0.05$;

Setting II : A compound Poisson process with uniform distributed demands and the corresponding Lévy measure is $\nu(dx) = \lambda/(2\beta)dx,\ x \in [0, 2\beta]$, where $\beta = \mu_\nu/\lambda$ and the Poisson intensity is $\lambda = 1$;

Setting III : A compound Poisson process with a mixture of Erlang demands and the Lévy measure is $\nu(dx) = \lambda(q_1\theta e^{-\theta x} + q_2\theta^2 x e^{-\theta x})dx,\ x \geq 0$, where $\{q_1, q_2\} = \{0.8, 0.2\},\ \theta = 0.5$, and the Poisson intensity is $\lambda = \frac{\theta\mu_\nu}{q_1+2q_2}$;

Setting IV : A Gamma process as specified in Example EC.2 and the corresponding Lévy measure is $\nu(dx) = (\alpha e^{-\beta x}/x)dx$ for $x > 0$, where $\alpha = 0.8$ and $\beta = 0.04$;

Setting V : An inverse Gaussian process as specified in Example EC.3 and the corresponding Lévy measure is $\nu(dx) = \frac{\delta}{\sqrt{2\pi x^3}} e^{-\frac{\gamma^2 x}{2}}dx$ for $x > 0$, where $\delta = 1$ and $\gamma = 0.05$.

The optimal replenishment rates and corresponding total discounted costs under these five settings are presented in Table EC.8. We observe that with different choices of demand dynamics but with the same mean, the optimal replenishment rates could significantly differ. Even with the same mean, the jump intensities and demand distribution are diverse for different dynamics. Consequently, the corresponding lost-sales frequencies and sizes also have a large difference, as does the total cost. These results positively answer the influence of different demand dynamics on the optimal replenishment rate. Therefore, choosing appropriate dynamics to model the random demands is critical. In this respect, our framework provides high flexibility in solving the optimal

replenishment rate for various demand dynamics. Finally, we present the corresponding studies in Table EC.9 when the cost functions are $h(x) = \sqrt{x}$ and $w(x) = 10(1 - e^{-\xi x})$. Similar observations can be made accordingly.

Table EC.8 Optimal quantities for selected demand dynamics under settings I-V.

	Setting I			Setting II			Setting III			Setting IV			Setting V		
u	ξ^*	ρ^*	$\Phi_{\rho^*}(u)$	ξ^*	ρ^*	$\Phi_{\rho^*}(u)$	ξ^*	ρ^*	$\Phi_{\rho^*}(u)$	ξ^*	ρ^*	$\Phi_{\rho^*}(u)$	ξ^*	ρ^*	$\Phi_{\rho^*}(u)$
0	0.0405	13.5279	694.43	0.0344	16.1843	747.52	0.0236	23.1938	871.07	0.0295	18.379	780.94	0.0589	6.7381	466.62
5	0.0414	13.348	684.42	0.0349	16.086	739.55	0.0252	22.8486	741.40	0.0307	18.1076	741.48	0.0678	6.2195	431.79
10	0.0426	13.1465	676.91	0.0354	15.9547	731.40	0.0276	22.4122	661.70	0.0318	17.8662	722.13	0.0727	5.9757	430.76
15	0.0439	12.9259	671.68	0.0362	15.7872	723.29	0.0303	21.9759	614.02	0.033	17.6204	710.03	0.0771	5.7808	436.50
20	0.0454	12.6886	668.58	0.0372	15.5813	715.55	0.0332	21.5664	587.12	0.0342	17.3695	702.89	0.0813	5.6128	446.20
25	0.047	12.4365	667.44	0.0384	15.3364	708.63	0.0363	21.1882	574.30	0.0356	17.1143	699.66	0.0853	5.4628	458.67
30	0.0488	12.1715	668.13	0.0399	15.0546	703.18	0.0395	20.8392	571.45	0.037	16.8561	699.65	0.0893	5.3261	473.28
40	0.0529	11.6081	674.43	0.0433	14.4252	700.73	0.0462	20.2131	585.84	0.0402	16.3339	707.59	0.0971	5.0823	507.45
50	0.0578	11.008	686.49	0.0473	13.761	709.54	0.0533	19.6595	617.59	0.0437	15.809	724.10	0.1049	4.8681	546.78

Table EC.9 Optimal quantities for selected demand dynamics under settings I-V with $h(x)=\sqrt{x}$, $w(x)=10(1-e^{-x})$, and $\mu_\nu=20$.

	Setting I			Setting II			Setting III			Setting IV			Setting V		
u	ξ^*	ρ^*	$\Phi_{\rho^*}(u)$	ξ^*	ρ^*	$\Phi_{\rho^*}(u)$	ξ^*	ρ^*	$\Phi_{\rho^*}(u)$	ξ^*	ρ^*	$\Phi_{\rho^*}(u)$	ξ^*	ρ^*	$\Phi_{\rho^*}(u)$
0	0.0318	15.3802	90.3890	0.0257	18.4827	94.3695	0.0150	26.0013	109.8974	0.0203	21.1151	99.7255	0.0478	7.5985	72.3428
5	0.0325	15.2039	89.7219	0.0260	18.3960	93.8894	0.0170	25.1097	95.9150	0.0214	20.6760	95.6761	0.0573	6.8478	68.2977
10	0.0334	14.9895	89.1154	0.0265	18.2580	93.1586	0.0196	24.2287	87.5807	0.0224	20.3381	93.7442	0.0610	6.6045	68.4860
15	0.0344	14.7554	88.6482	0.0271	18.0769	92.3979	0.0223	23.4898	82.9932	0.0234	20.0216	92.5677	0.0639	6.4298	69.1971
20	0.0355	14.5069	88.3185	0.0278	17.8544	91.6280	0.0251	22.8777	80.4594	0.0244	19.7157	91.8169	0.0665	6.2894	70.1535
25	0.0368	14.2471	88.1187	0.0287	17.5926	90.8927	0.0279	22.3622	79.2010	0.0254	19.4180	91.3740	0.0687	6.1702	71.2534
30	0.0381	13.9784	88.0386	0.0298	17.2964	90.2517	0.0307	21.9196	78.7905	0.0265	19.1277	91.1745	0.0708	6.0657	72.4467
40	0.0410	13.4201	88.1954	0.0324	16.6541	89.6031	0.0363	21.1879	79.5505	0.0287	18.5677	91.3393	0.0747	5.8873	75.0096
50	0.0444	12.8416	88.7107	0.0352	16.0169	89.8875	0.0420	20.5934	81.5410	0.0310	18.0332	92.0731	0.0782	5.7370	77.7141

EC.3.3. Accelerated Fourier-cosine Method

Although many Fourier inversion methods exist (see, e.g., Fang and Oosterlee 2009 and Li et al. 2021), a typical Fourier-based method involves applying a summation or an integration of trigonometric functions to approximate the target function, where oscillation naturally arises with a different number of terms used in approximation. To eliminate the oscillation in convergence, we adopt different filters to accelerate our Fourier-cosine method.

Specifically, we consider a truncated Fourier expansion of $f(x)$ with $2N+1$ terms as below:

$$f(x) = \sum_{n=-\infty}^{\infty} c_n \exp(inx) \approx f_N(x) := \sum_{n=-N}^{N} c_n \exp(inx).$$

We introduce several different accelerating filters in computing this summation in what follows. A linear-sum acceleration filter $\sigma(\theta)$ is defined to be an even function with $\sigma(0)=1$, where the corresponding filtered partial sum is given by (Boyd 2011)

$$f_N^{\sigma}(x) = \sum_{n=-N}^{N} \sigma(j/N) c_n \exp(inx).$$

Furthermore, we recall that our Fourier-cosine method treats the cosine functions as basis functions. Therefore, some extant filters should particularly suit our formulation, and we here introduce three popular options, i.e., the Euler filter (Wimp 1981), the Erfc-log filter (Boyd 1996), and the HDAF filter (Tanner 2006), with the corresponding filtering function defined as follows:

1. Euler filter: $\sigma_{Euler}\left(\frac{j}{N}\right) = \sum_{l=j}^{N} \frac{1}{2^N}\binom{N}{l}, j=0,1,\ldots,N$;

2. Erfc-log filter: $\sigma_{Erfc-log}(\kappa;p) = \frac{1}{2}\text{erfc}\left\{2p^{\frac{1}{2}}\kappa'\sqrt{\frac{-\ln(1-4\kappa'^2)}{4\kappa'^2}}\right\}$, where $\kappa' = |\kappa| - \frac{1}{2}$, $\text{erfc}(\cdot)$ is the complementary error function defined by $\text{erfc}(z) = \frac{2}{\sqrt{\pi}}\int_z^{\infty} e^{-t^2}dt$ and p is a function of the independent variable x through $p(x) = 1 + \frac{N|x|}{2\pi}$;

3. HDAF filter: $\sigma_{HDAF}(\kappa) = \exp(-N|x|\kappa^2/2)\sum_{j=0}^{\left\lfloor \frac{N|x|}{15} \right\rfloor} \frac{(N|x|\kappa^2/2)^j}{j!}$, where $\lfloor x \rfloor$ is the largest integer not exceeding x.

To apply an acceleration filter $\sigma(\kappa)$ in our Fourier-cosine approximation (17) of $\Phi_\rho(u)$, we have

$$\Phi_\rho(u) \approx e^{ku}\left[\sum_{j=0}^{J}{}'\sigma(j/J)F_j\cos\left(\frac{j\pi}{a}u\right)\right].$$

We first examine the performance of these filters in the convergence speed in terms of J in Figure EC.7. The model settings are the same as in Example EC.1, with the parameters being $\lambda = 1$, $\mu_\nu = 2$, $u = 10$, and $k = 0.05$. The Euler filter performs even worse than the original Fourier-cosine method without any filter. In contrast, the Erfc-log filter performs best among these methods, where the approximation quickly converges to the reference value without oscillation. Under the HDAF filter, though the approximation also converges very fast, it is not that stable as there appears to be a sudden jump.

We then check the robustness of the filtered Fourier-cosine schemes in the choice of a and make a plot on $\Phi_{\rho^*}(u)$ against a in Figure EC.8 with a fixed $J = 2^9$ and the same parameter settings as in Figure EC.7. We observe that the Euler filter can help to reduce oscillation when a is relatively small. Still, it aggravates the oscillation when a becomes large. On the other hand, both the Erfc-log filter and HDAF filter can effectively eliminate the oscillation and consistently achieve accuracy by converging to the reference value before a reaches our suggested value, as shown in Figure EC.8. The corresponding approximation errors with our suggested a are provided in Table EC.10 for a better comparison. Therefore, in terms of stability and robustness, our numerical experiments conclude that our Fourier-cosine method, combined with the Erfc-log filter, as shown in (21), achieves the best results.

Figure EC.7 The discounted cost $\Phi_{\rho^*}(u)$ for different filters.

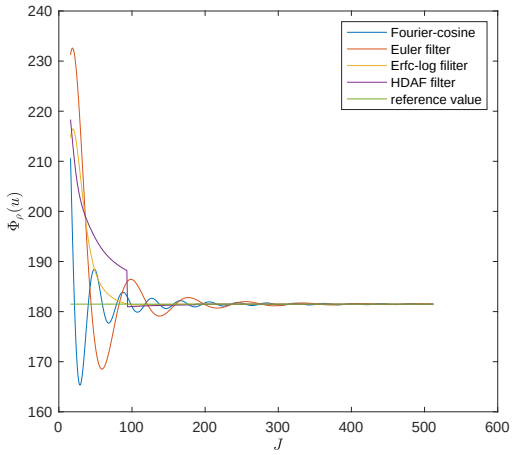

Figure EC.8 The discounted cost $\Phi_{\rho^*}(u)$ for different filters.

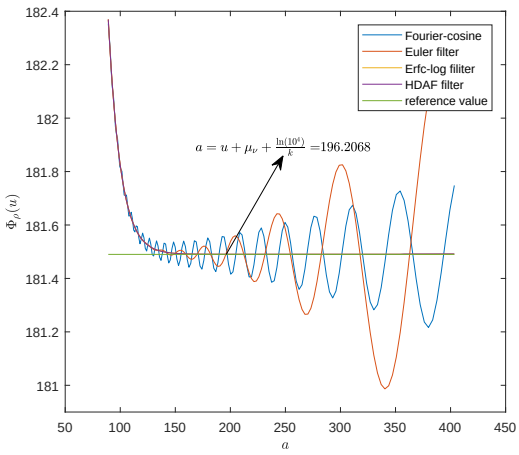

Table EC.10 $\Phi_{\rho^*}(u)$ for compound Poisson demands with exponential sizes under different filters.

$\Phi_{\rho^*}(u)$	reference	Fourier-cosine	Euler	Erfc-log	HDAF
$\Phi_{\rho^*}(5)$	193.450	193.3569	193.6778	193.4488	193.4488
$\Phi_{\rho^*}(10)$	181.490	181.5161	181.4940	181.4906	181.4906
$\Phi_{\rho^*}(15)$	191.810	191.8507	191.8076	191.8075	191.8075
$\Phi_{\rho^*}(20)$	212.640	212.5777	212.6426	212.6420	212.6420
$\Phi_{\rho^*}(25)$	239.160	239.2379	239.1562	239.1562	239.1562
$\Phi_{\rho^*}(30)$	269.040	269.0012	269.0391	269.0391	269.0391
$\Phi_{\rho^*}(40)$	334.520	334.6763	334.5168	334.5168	334.5168
$\Phi_{\rho^*}(50)$	404.150	404.4242	404.1479	404.1479	404.1479

EC.3.4. Connections with the Bromwich Integral

We now briefly compare our Fourier-cosine scheme with the inverse Laplace method for completeness. On the one hand, there is an intimate connection between these two methods. For an arbitrary real function $f(x)$ on $x \in [0,\infty)$ satisfying certain integrability conditions, the Fourier transform of $\bar{f}(x) := e^{-kx} f(x)$, i.e., $[\mathcal{F}\bar{f}](s)$, is precisely the Laplace transform of $f(x)$ with the frequency variable replaced by $k+is$, i.e., $\tilde{f}(k+is)$. We recall that Mellin's formula for the inverse Laplace transform, also called the Bromwich integral, is given by (Abate and Whitt 2006)

$$f(x) = \mathcal{L}^{-1}\{\tilde{f}\}(x) = \frac{1}{2\pi i} \lim_{T\to\infty} \int_{\gamma-iT}^{\gamma+iT} e^{tx} \tilde{f}(t) dt. \tag{EC.41}$$

Consequently, the Fourier-cosine approximation in $\tilde{f}(k+is)$ resembles numerically computing the Bromwich integral by letting $\gamma = k$. By a change of variable $t = \gamma + is = k + is$, we have

$$f(x) = \frac{1}{2\pi i} \int_{k-i\infty}^{k+i\infty} e^{xt} \tilde{f}(t) dt = e^{kx} \frac{1}{2\pi} \int_{-\infty}^{+\infty} e^{isx} \tilde{f}(k+is) ds. \tag{EC.42}$$

Since $f(x)$ is a real function whose imaginary part is 0, and if we further assume that $f(-x) = 0$ for $x > 0$, we can then rewrite (EC.42) as

$$\begin{aligned} f(x) &= e^{kx} \frac{1}{2\pi} \left[\int_{-\infty}^{+\infty} \cos(sx) \Re\{\tilde{f}(k+is)\} ds - \int_{-\infty}^{+\infty} \sin(sx) \Im\{\tilde{f}(k+is)\} ds \right] \\ &= e^{kx} \frac{2}{\pi} \int_{0}^{+\infty} \cos(sx) \Re\{\tilde{f}(k+is)\} ds. \end{aligned} \tag{EC.43}$$

Incidentally, our Fourier-cosine approximation coincides with a trapezoidal rule of (EC.43):

$$\begin{aligned}\Phi_\rho(x) &\approx e^{kx}\sum_{n=0}^{J}{}'\frac{2}{a}\Re\left\{\tilde{\tilde{\Phi}}_\rho\left(i\frac{n\pi}{a}\right)\right\}\cos\left(\frac{n\pi}{a}x\right)\\ &= e^{kx}\left[\frac{1}{a}\Re\left\{\tilde{\Phi}_\rho(k)\right\}+\frac{2}{a}\sum_{n=1}^{J}\Re\left\{\tilde{\Phi}_\rho\left(k+i\frac{n\pi}{a}\right)\right\}\cos\left(\frac{n\pi}{a}x\right)\right]\end{aligned}$$

In other words, the Fourier-cosine method with an appropriate filter described in Section EC.3.3 can even better approximate a Bromwich integral (Abate and Whitt 2006).

On the other hand, the inverse Laplace method could usually be unstable in numerical approximations and untraceable in error analysis. In contrast, our Fourier-cosine method can overcome these deficiencies effectively, as shown in the previous sections. Some common ideas in evaluating the Bromwich integral include representing it by combining Gaver functionals and deforming its contour (Abate and Whitt 2006). Due to the limited machine precision, the round-off error could dramatically increase when people attempt to increase the computational accuracy, which often makes the inverse Laplace schemes numerically unstable. To illustrate this, we examine the Talbot algorithm, one of the most popular inverse Laplace schemes.

Specifically, the Talbot algorithm deforms the standard contour in s (see (EC.41)) to z through a transform $s = S_v(z)$, where the family of contours $\{v : S_v(z)\}$ is given by

$$S_v(z) = \frac{z}{1-e^{-z}} + \frac{v-1}{2}z.$$

Indeed, the Talbot algorithm must manually determine many parameters in the discretization and truncation processes. The settings of these parameters heavily rely on the locations of singular points of $\tilde{f}$. For convenience, we consider the simplified Talbot algorithm proposed by Abate and Whitt (2006) that has only one parameter J, and it is of the form

$$f_M(t) = \frac{1}{t}\sum_{j=0}^{J}\omega_j\tilde{f}\left(\frac{\alpha_j}{t}\right).$$

It turns out to converge very fast in most cases. However, if we desire to improve the approximation accuracy and increase the number of summation terms J, the previously mentioned problem of

increased round-off errors could significantly influence its final precision. To see this, we present some numerical experiments to compare our filtered Fourier-cosine scheme using the Erfc-log filter with the simplified Talbot algorithm. The demand dynamics is assumed to be a Gamma process with $\alpha = 0.8$, $\beta = 0.4$, and therefore, $\mu_\nu = 2$. We set $u = 10$ and $r = 0.1$. Using our accelerated Fourier-cosine method, the minimum cost is 146.7411, at $\xi^* = 0.2315$. With this optimal ξ^*, we plot the total cost $\Phi_\rho(u)$ against different choices of J using the Talbot algorithm in Figure EC.9. We can see that the Talbot method gets the correct answer with a small J. However, if we want to improve the approximation accuracy and increase J to 80 or above, the approximation gets out of control, and its solution is fallacious. In contrast, using our accelerated Fourier-cosine method, one can achieve an arbitrary accuracy by increasing a and J.

Figure EC.9 The discounted cost $\Phi_\rho(u)$ in comparing the Talbot algorithm and our method.

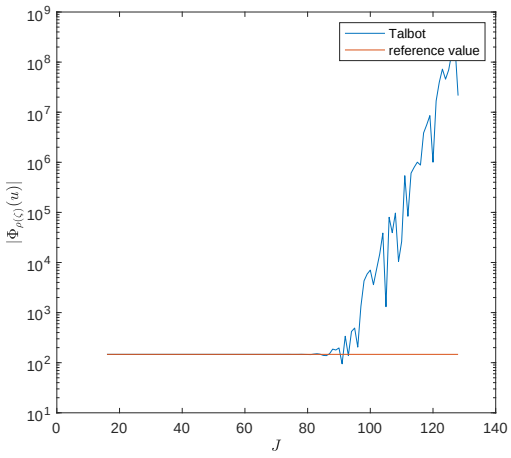

EC.4. Numerical Experiments II: Risk Analytics and Constrained Production Planning

We here illustrate the application of the proposed Fourier-cosine method in calculating the risk analytics discussed in Section 5. Furthermore, we consider the associated constrained production planning problem when some restrictions regarding these risk analytics are required.

EC.4.1. Finite-Time Stockout Probability

We respectively compute $\phi_u(T)$ in two demand instances, i.e., a compound Poisson process with a finite Lévy measure and a Gamma process with an infinite Lévy measure. Specifically, as noted in

Remark 1(c), we need to set a proper L to determine an appropriate truncation parameter a. We also check the robustness of numerical results in choosing L.

First, let $D(t)$ be a compound Poisson process with exponentially-distributed demands, where the intensity $\lambda = 1$ and the exponential rate $\mu = 1$. We then have $\mu_\nu = \lambda/\mu = 1$. Using the approximation formula (25) in Theorem 3, we plot the stockout probability $\phi_u(T)$ against u in Figure EC.10. For the other parameters in the model and Fourier-cosine scheme, we choose $\rho = 1.5$, $T = 10$, $J = 512$, $L = 10$, and $n_0 = 0$. To show the precision of our approximation, we also perform Monte Carlo simulations (with 10^4 samples) 30 times for each u and construct a highlighted band representing the 95% confidence intervals. Unsurprisingly, the stockout probability is monotonically decreasing in the initial inventory. Furthermore, we test the robustness of the calculation with respect to L in Figure EC.11 under the same parameter setting, except that the initial inventory u is fixed at 1, and L varies now. We plot a similar highlighted band using standard Monte Carlo simulations. It turns out that the numerical result is very robust to the choice of L (i.e., a via (26)), provided that the truncation domain is reasonably large, say L is greater than 2.

Figure EC.10 The stockout probability $\phi_u(T)$ for a compound Poisson process with exponential demands.

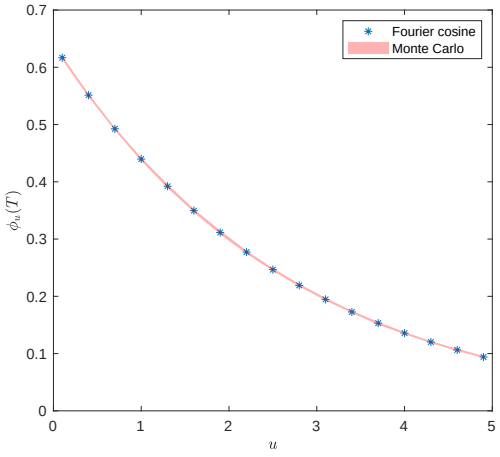

Figure EC.11 The stockout probability $\phi_u(T)$ for a compound Poisson process with exponential demands.

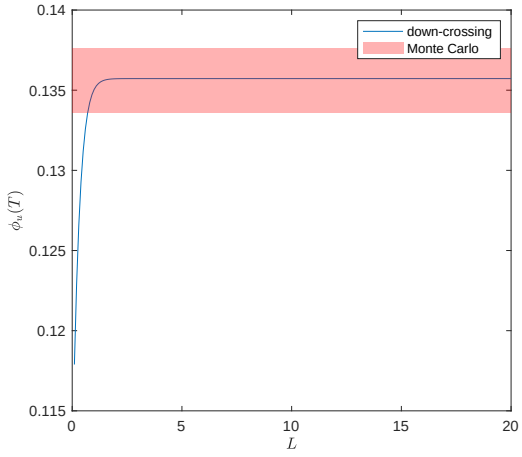

We next examine the numerical performance under an alternative Gamma demand process. Let D_t now be a Gamma process with parameters $\alpha = 0.8$, $\beta = 0.4$, and therefore, $\mu_\nu = \alpha/\beta = 2$. Other

parameters are $\rho = 1.5$, $T = 10$, and $J = 512$. With a fixed L at 10, we plot $\phi_u(T)$ versus the initial inventory u in Figure EC.12 with two options of n_0 equal to 0 or 1. Compared to the Monte Carlo results in Dufresne et al. (1991), the approximation is always accurate. A closer examination of the robustness test in L reveals that when $n_0 = 1$, the convergence is comparatively more steady. The comparatively less stable approximation for the setting $n_0 = 0$ may be because the density function of a Gamma process is divergent at some singular points. See Section 5.1.1 for a more detailed discussion on adding the factor x^{n_0}.

Figure EC.12 The stockout probability $\phi_u(T)$ for a Gamma demand.

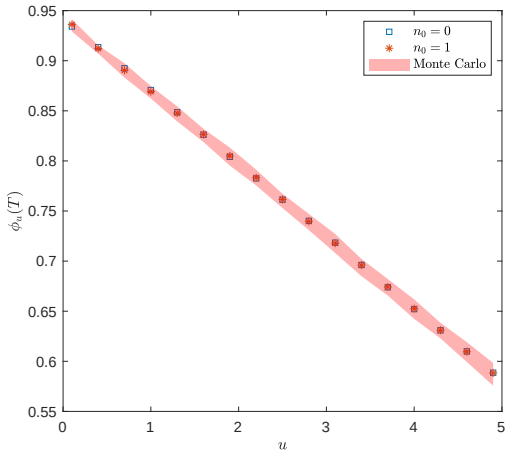

Figure EC.13 The stockout probability $\phi_u(T)$ for a Gamma demand.

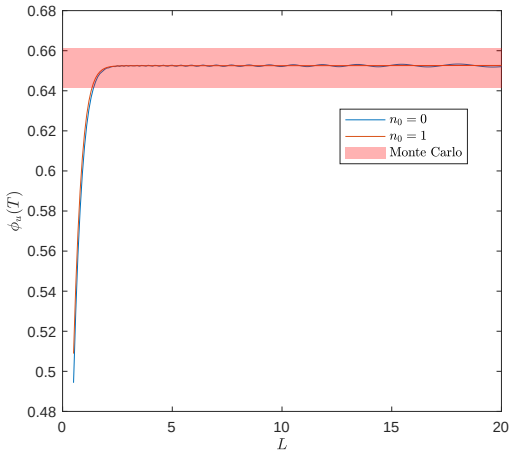

EC.4.2. Expected Time to Stockout

We use the compound Poisson and Gamma cases to illustrate the numerical performance in calculating $\varphi(u)$. Under the compound Poisson demand, $\varphi(u)$ is explicitly given by $\varphi(u) = \frac{\mu u+1}{\rho \xi_0}$. Other model parameters are set as $\lambda = 1$, $\mu = 1$, $\rho = 0.2, J = 512$, and $k = 0.1$. The numerical results match the exact values, as shown in Figure EC.14.

In the Gamma case, however, a closed-form expression for $\varphi(u)$ is no longer available. The parameters are set to be $\alpha = 0.8$, $\beta = 0.4$, $\rho = 0.2$, $J = 512$, and $k = 0.1$. The corresponding plots are in Figures EC.16 and EC.17, where the Monte Carlo bands are obtained similarly to the previous section. We can observe that the numerical performance of the Fourier-cosine method is stable and accurate, as expected.

Figure EC.14 The expected stockout time $\varphi(u)$ for a compound Poisson process with exponential demands.

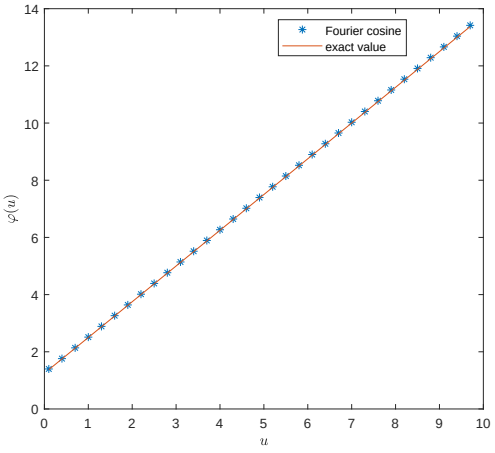

Figure EC.15 The expected stockout time $\varphi(u)$ for a compound Poisson process with exponential demands.

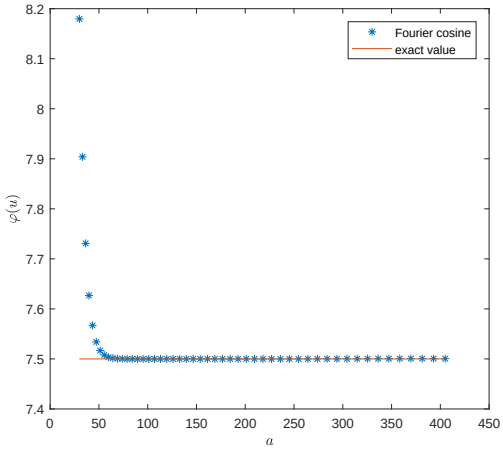

Figure EC.16 The expected stockout time $\varphi(u)$ for a Gamma demand process.

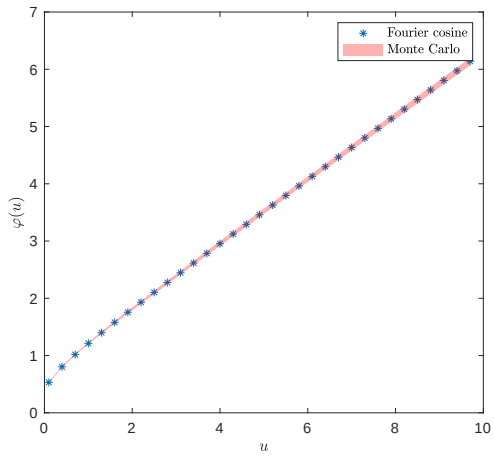

Figure EC.17 The expected stockout time $\varphi(u)$ for a Gamma demand process.

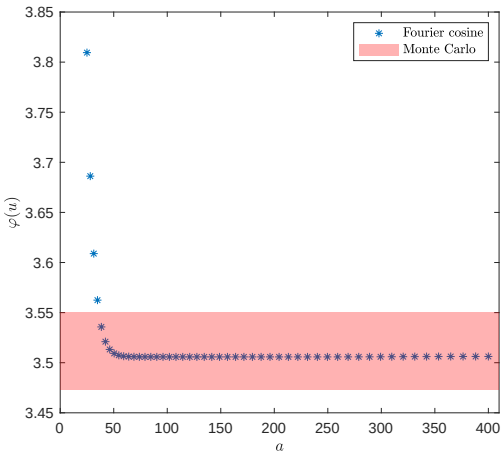

EC.4.3. Expected Size of Stockout

The same parameter settings as in Section EC.4.2 are adopted here. Specifically, we have $\mathcal{L}_\tau(u) = 1/\mu$ under the compound Poisson case, indicating that it only depends on the expected size of each arrival demand. Figure EC.18 confirms that $\mathcal{L}_\tau(u)$ is constant with different values of the initial level u. Nevertheless, Figure EC.20 shows that the expected stockout size is increasing in the initial inventory level for Gamma demands.

Figure EC.18 The expected stockout size $\mathcal{L}_\tau(u)$ for a compound Poisson process with exponential demands.

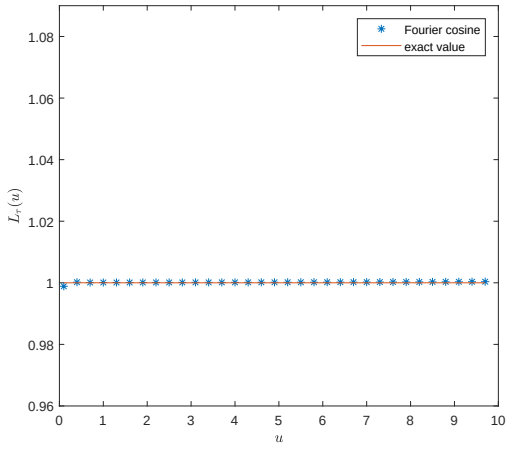

Figure EC.19 The expected stockout size $\mathcal{L}_\tau(u)$ for a compound Poisson process with exponential demands.

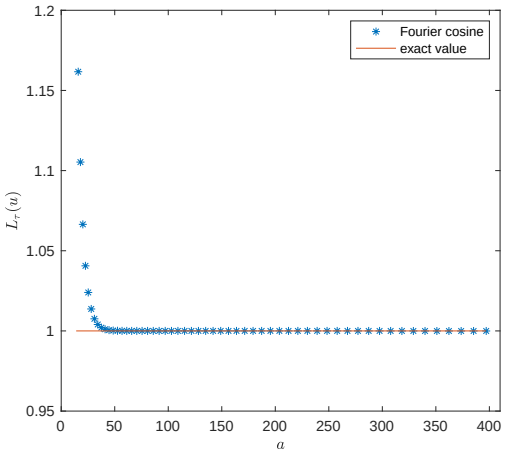

Figure EC.20 The expected stockout size $\mathcal{L}_\tau(u)$ for a Gamma demand process.

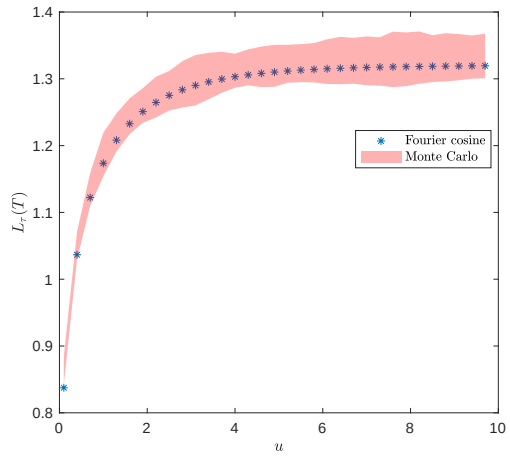

Figure EC.21 The expected stockout size $\mathcal{L}_\tau(u)$ for a Gamma demand process.

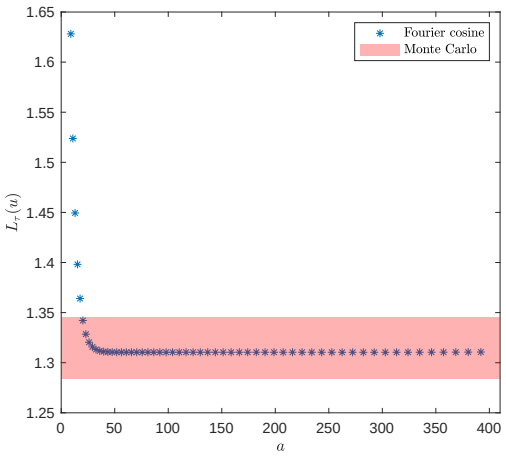

EC.4.4. Production Planning with Constraints on Stockout Risks

Finally, we illustrate how to solve the constrained total discounted cost minimization problem that incorporates the risk analytics as the constraints in two demand instances, i.e., a compound Poisson process with a finite Lévy measure (distributional setting: $\lambda = 1, \mu = 0.5, \mu_\nu = \lambda/\mu = 2$) and a Gamma process with an infinite Lévy measure (distributional setting: $\alpha = 0.8, \beta = 0.4, \mu_\nu = \alpha/\beta = 2$). Specifically, Proposition 9 indicates that we can effectively solve the constrained produc-

tion planning problem by first finding the cutoff point corresponding to each constraint and then comparing the cutoff point with the previous solution to the unconstrained optimization problem.

Under the constraint (P1), we consider $\phi_u(T) \le c_1$ and let $u = 10, T = 10, c_1 = 0.1, r = 0.1$, and $k = 0.05$. The corresponding plots for finite-time stockout probability and total discounted cost against the production rate in these two examples are given in Figures EC.22 and EC.23, respectively. Specifically, the left axis labels the total discounted cost $\Phi_\rho(u)$, the right axis represents the finite-time stockout probability $\phi_u(T)$, and the dotted line divides the searching area of the production rate into two separate parts, with its right-hand side being the desired region such that the stockout probability is below the threshold c_1. In Figure EC.22, it is clear that the previous unconstrained solution ($\rho^* = 2.17$) is no longer attainable when the constraint (P1) is imposed. Instead, the cutoff point of $\phi_u(T) = c_1$ is $\rho = 2.8883$, which becomes the optimal production rate of the constrained optimization problem. Figure EC.23 shows that the cutoff point of $\phi_u(T) \le c_1$ is $\rho = 2.3016 > \rho^* = 2.0099$, which is the optimal production rate for this constrained problem.

Figure EC.22 Constraint on $\phi_u(T)$ for a compound Poisson process with exponential demands.

Figure EC.23 Constraint on $\phi_u(T)$ for a Gamma demand process.

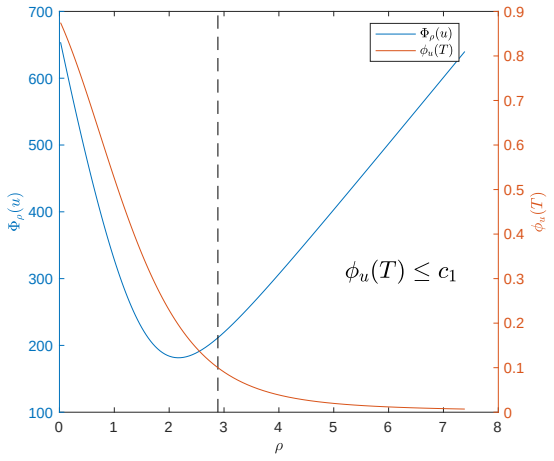

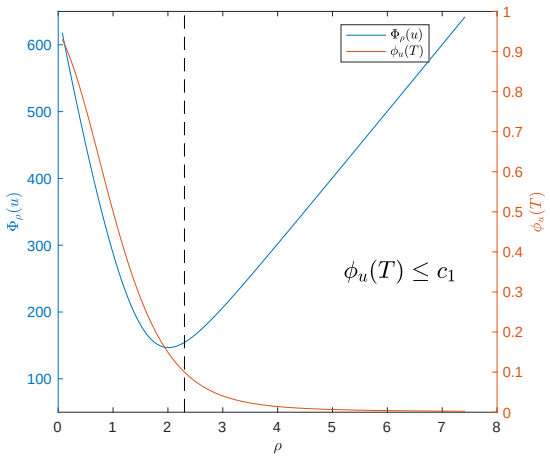

Under the constraint (P2) where $\varphi(u) \ge c_2$, we consider the following parameter set for an example: $u = 10, T = 10, c_2 = 15, r = 0.1$, and $k = 0.05$. Similar plots for the compound Poisson process and the Gamma process are in Figures EC.24 and EC.25, respectively. In these figures, the

right axis corresponds to the expected stockout time $\varphi(u)$, and the right-hand side of the dotted line denotes the set of production rates that fulfill the constraint on stockout time. Unlike Figures EC.22 and EC.23, the unconstrained solution now falls within the constrained sets in Figures EC.24 and EC.25. Therefore, the optimal constrained solution is identical to the unconstrained one. Specifically, the optimal production rates for the constrained and unconstrained optimization problems are 2.1700 in Figure EC.24 and 2.0099 in Figure EC.25.

Figure EC.24 Constraint on $\varphi(u)$ for a compound Poisson process with exponential demands.

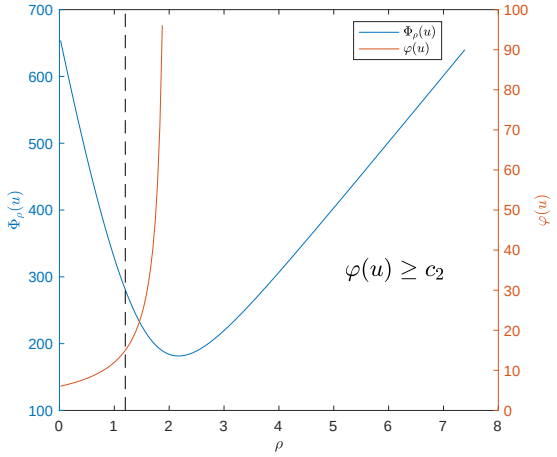

Figure EC.25 Constraint on $\varphi(u)$ for a Gamma demand process.

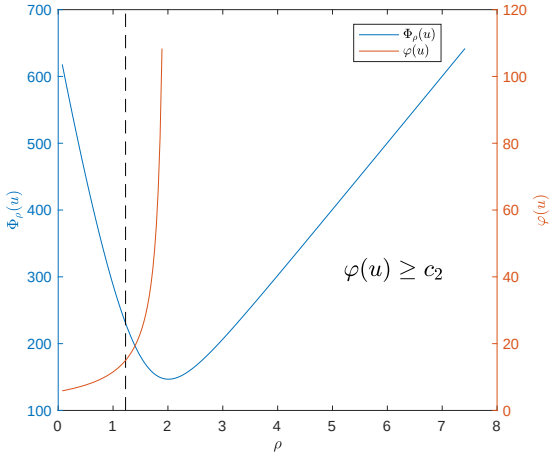

For the last example, we consider the constraint (P5) such that $l \leq c_5$. Let $u = 10, T = 10, c_2 = 0.5, r = 0.1$, and $k = 0.05$. The corresponding plots for the two demand cases are in Figures EC.26 and EC.27, respectively. The right axis represents the long-run lost demand percentage l, while the left is the total discounted cost. Therefore, the current constraint renders the searching area of the production rate to be the right-hand side of the dotted line. A similar argument gives the optimal production rate 2.1700 for both the unconstrained and constrained optimization problems in Figure EC.26, while it is 2.0099 in Figure EC.27.

References

Abate, J., Whitt, W. 2006. A unified framework for numerically inverting Laplace transforms. *INFORMS Journal on Computing,* 18 (4), 408–421.

Asmussen, S., Albrecher, H. 2010. *Ruin probabilities.* Vol. 14, World Scientific.

Figure EC.26 Constraint on l for a compound Poisson process with exponential demands.

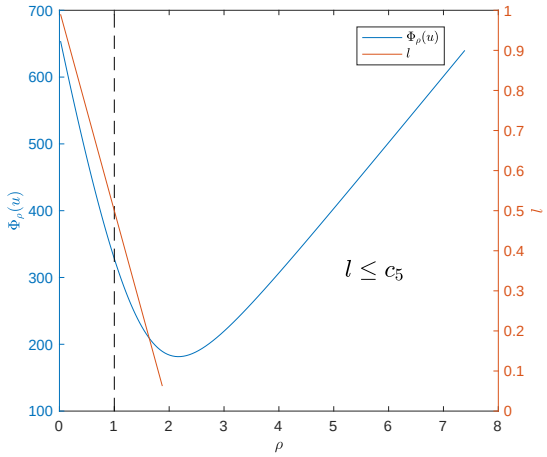

Figure EC.27 Constraint on l for a Gamma demand process.

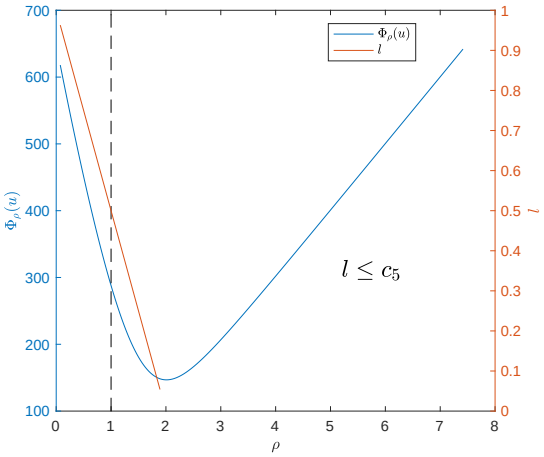

Bertsimas, D., Tsitsiklis, J. 1993. Simulated annealing. *Statistical Science,* 8 (1), 10–15.

Boyd, J.P. 1996. The erfc-log filter and the asymptotics of the Euler and Vandeven sequence accelerations. *Proceedings of the Third International Conference on Spectral and High Order Methods,* 267–276.

Boyd, J.P. 2001. *Chebyshev and Fourier spectral methods.* Courier Corporation.

Boyd, J.P. 2011. A proof, based on the Euler sum acceleration, of the recovery of an exponential (geometric) rate of convergence for the Fourier series of a function with Gibbs phenomenon. *Spectral and High Order Methods for Partial Differential Equations,* 131–139.

Cai, J., Feng, R., Willmot, G.E. 2009. On the expectation of total discounted operating costs up to default and its applications. *Advances in Applied Probability,* 41(2), 495–522.

D'Auria, B., Samorodnitsky, G. 2005. Limit behavior of fluid queues and networks. *Operations Research,* 53(6), 933–945.

Erdélyi, A. 1955. Asymptotic representations of Fourier integrals and the method of stationary phase. *Journal of the Society for Industrial and Applied Mathematics,* 3 (1), 17–27.

Erdélyi, A. 1956. Asymptotic expansions of Fourier integrals involving logarithmic singularities. *Journal of the Society for Industrial and Applied Mathematics,* 4 (1), 38–47.

Fang, F., Oosterlee, C.W. 2009. A novel pricing method for European options based on Fourier-cosine series expansions. *SIAM Journal on Scientific Computing,* 31(2), 826–848.

Forrest, S. 1993. Genetic algorithms: principles of natural selection applied to computation. *Science,* 261(5123), 872–878.

Gerber, H. U., Shiu, E.S.W. 1997. The joint distribution of the time of ruin, the surplus immediately before ruin, and the deficit at ruin. *Insurance: Mathematics and Economics,* 21(2), 129–137.

Hansen, E., Walster, G.W. 2003. *Global optimization using interval analysis: revised and expanded.* Vol. 264, CRC Press.

Hewitt, E., Hewitt, R.E. 1979. The Gibbs-Wilbraham phenomenon: an episode in Fourier analysis. *Archive for history of Exact Sciences,* 129–160.

Kella, O., Whitt, W. 1992. Useful martingales for stochastic storage processes with Lévy input. *Journal of Applied Probability,* 29(2), 396–403.

Kyprianou, A.E. 2014. *Fluctuations of Lévy processes with applications: Introductory Lectures.* Springer Science & Business Media, New York.

Li, X., Shi, Y., Yam, S.C.P., Yang, H. 2021. Fourier-cosine method for finite-time Gerber–Shiu functions. *SIAM Journal on Scientific Computing,* 43(3), B650–B677.

Morales, M. 2007. On the expected discounted penalty function for a perturbed risk process driven by a subordinator. *Insurance: Mathematics and Economics,* 40(2), 293–301.

Ross, S. M. 1996. *Stochastic Processes*, 2nd ed. John Wiley & Sons, New York.

Shi, J., Katehakis, M. N., Melamed, B., Xia, Y. 2014. Production-inventory systems with lost sales and compound Poisson demands. *Operations Research,* 62 (5), 1048–1063.

Tanner, J. 2006. Optimal filter and mollifier for piecewise smooth spectral data. *Mathematics of Computation,* 75 (254), 767–790.

van Noortwijk, J.M. 2009. A survey of the application of gamma processes in maintenance. *Reliability Engineering & System Safety,* 94 (1), 2–21.

Wimp, J. 1981. *Sequence transformations and their applications*, Academic Press, New York.

Wong, R., Lin, J. 1978. Asymptotic expansions of Fourier transforms of functions with logarithmic singularities. *Journal of Mathematical Analysis and Applications,* 64 (1), 173–180.